東海大學生命科學系

碩士論文

指導教授: 謝明麗 博士

Mingli Hsieh, Ph.D

碳酸酐酶蛋白八與脊髓小腦共濟失調症第三型的角色

Roles of the carbonic anhydrase 8 in spinocerebellar ataxia type 3

研究生: 李依庭

Yi-Ting Li

中華民國一〇四年七月

致謝

在東海大學求學六年中，有著許多人的幫助與鼓勵，感謝那些曾經幫助我的師長與同儕，讓我能夠完成實驗以及這本論文。

從剛進入大學懵懵懂懂的我，在大二加入了實驗室之後，感謝實驗室的老師、學長、學姊、學弟、學妹的教導或幫助，使我能夠專心於研究中，讓我對於自然的探索有更深的體悟，也習得許多寶貴的實驗技術；在求學過程中或許發生了許多意想不到的驚喜或驚嚇，但對於我來說都是不可多得的經驗，感謝從大學一路幫助過我的人，不論是開心還是挫折，都有幸與你們同在。

除了師長與同儕，更要感謝我的家人，有你們默默地在背後支持，我才能夠無後顧之憂地在研究上全力以赴，順利完成這本論文。

最後我也謝謝我自己，努力不一定會有回報，但不努力一定不會有滿滿的收穫的，縱使人生的路還很漫長，加油。

摘要

脊髓小腦共濟失調症第三型(Spinocerebellar ataxia type 3, SCA3)/ 馬查多-約

瑟夫病 (Machado–Joseph disease, MJD)是一種神經退化性疾病，屬於晚發型的

疾病。此疾病的突變蛋白 (mutant ataxin-3)在基因序列上帶有一段不正常的三核

甘酸 CAG 擴增(大於 52 次)所導致，這段 CAG 序列會轉譯出不正常擴增的多醯

麩氨酸蛋白(poly Q)。這類不正常擴增的多醯麩氨酸蛋白會沉積在小腦當中，在

病理上會造成小腦萎縮。此外，在先前的文獻也顯示此疾病與三磷酸肌醇受體

(IP_3R1)蛋白有交互作用並且會增加不正常的鈣離子釋放。而在我們實驗室先前的

研究發現當碳酸酐酶 VIII(CA8)在人類神經母細胞瘤表達此突變蛋白包含 78 次

的 CAG 序列 (SK-N-SH-MJD78)時，不論是在信使核糖核酸 (mRNA)或是蛋白

表現量都有明顯的上升。在我的實驗中，我在帶有 MJD 的轉殖小鼠小腦當中可

以觀察到與正常小鼠相比不論是在早期或晚期的 CA8 皆有明顯的上升。除此之

外，在突變的人類胚胎腎原細胞 (HEK293-MJD78)中發現會改變 CA8 的轉錄調

控。再者我利用在 SK-N-SH-MJD78 大量表現 CA8，透過組織免疫螢光染色

(immunofluorescence)和免疫共沉澱法 (immunoprecipitation)，發現 CA8 和 mutant

ataxin-3 會共表達 (co-localized)在細胞質內且產生交互作用。而當我在細胞中誘

發氧化壓力時，SK-MJD78-CA8 相較於 SK-MJD78-eGFP 細胞會有較高的存活度，

且較能夠抵抗細胞中的氧化壓力。我也發現不管是在 SK-MJD78-CA8 或突變小

鼠顆粒神經元 (Cerebellar granule neurons)在大量表達 CA8 後會減少不正常的鈣

離子釋放並且減少細胞死亡。其次，我們也發現當我們加藥 (A23187)誘發鈣離子後會削減 SK-MJD78-CA8 或突變小鼠顆粒神經元中 CA8 的保護功能。而在 SK-MJD78-CA8 或大量表達 CA8 的突變小鼠顆粒神經元中也發現葡萄糖攝取能力 (glucose uptake ability)相較於控制組有明顯的上升。總結目前的觀察，我希望能夠提供重要的訊息進一步釐清 CA8 和 mutant ataxin-3 的關係，並且提供一個未來可能的治療方向。

Abstract

Spinocerebellar ataxia type 3(SCA3)/Machado–Joseph disease (MJD), a late onset disease, is one of the neurodegenerative diseases. It is known that expansion of more than 52 times of CAG repeats encodes an abnormally long polyglutamine (polyQ) in the disease protein, mutant ataxin-3. Pathological hallmarks of the disease are cerebellar atrophy and neuronal intranuclear inclusions containing poly Q fragments in the cerebellum. It is noted that mutant ataxin-3 interacts with 1,4,5-trisphosphate receptor type 1(IP$_3$R1) and induces abnormal Ca^{2+} release. Our previous study showed a significant increase of the mRNA and protein expression of carbonic anhydrase VIII (CA8) in SK-N-SH-MJD78 cells, human neuroblastoma cells overexpressing mutant ataxin-3 with 78 glutamine repeats. In this study, we showed significantly altered CA8 expression in MJD mouse cerebellum in either early or late disease stage, as compared with its wild type control. Moreover, we demonstrated that the transcriptional regulation of CA8 was altered by mutant ataxin-3 in HEK293-MJD78 cells. In addition, we found that CA8 co-localized and interacted with mutant ataxin-3 in

SK-N-SH-MJD78 cells harboring overexpressing CA8 (SK-MJD78-CA8) by immunofluorescence and immunoprecipation analysis. Importantly, we showed that SK-MJD78-CA8 cells and mouse cerebellar granule neurons were more resistant to reactive oxygen species (ROS) stress than the control cells. Furthermore, we demonstrated that overexpression of CA8 in SK-MJD78-CA8 cells rescued the abnormal Ca^{2+} release observed in SK-MJD78 cells. Overexpression of CA8 in MJD cerebellum granule neurons decreased Ca^{2+} release and resulted in an increase in cell survival. Additionally, we found that Ca^{2+} ionophore A23187 counteracted the protective effect of CA8 in SK-MJD78-CA8 cells and MJD cerebellar granule neurons. Interestingly, the glucose uptake ability was significantly induced by overexpression of CA8 in SK-MJD78-CA8 cells and in MJD cerebellar granules neurons. Taken together, we demonstrate the protective function of CA8 in MJD disease models and our findings may provide important information for potential therapeutic targets in the future.

Content

Introduction

1.1 Machado-Joseph disease (MJD)/ Spinocerebellar ataxia type 3 (SCA3)

Machado–Joseph disease (MJD)/spinocerebellar ataxia type 3 (SCA3) is

an autosomal dominant neurodegenerative disease caused by poly

glutamine expanded ataxin-3. The main symptoms of MJD include

progressive ataxia, eye movement abnormalities, dysarthria, hyperreflexia,

dystonia and ophthalmoplegia (Coutinho and Andrade, 1978; Rosenberg,

1992; Soong et al., 1997). Previous neuropathological studies have

detected that neuronal loss in the cerebellum, midbrain, pons, medulla

oblongata and spinal cord in MJD patients (Riess et al., 2008). The MJD

disease gene was mapped to chromosome 14q32.1 (Kawaguchi et al.,

1994). Normal ataxin-3 contains 12~44 times glutamine repeats with a

molecular weight of approximate 42 kDa, whereas mutant ataxin-3

contains more than 52 times polyglutamine repeats (Kawaguchi et al.,

1994). Ataxin-3 is distributed in the cytoplasm and is able to translocate

from the cytoplasm to the nucleus and back (Chai et al., 2002). As for the

function of normal ataxin-3, it is a deubiquitinating enzyme (DUB) that

modulates substrate degradation through the ubiquitin–proteasome

pathway (Durcan and Fon, 2013). Another main function of ataxin-3 is capable of regulating the transcriptional process and interacting with numerous transcriptional regulators (Burnett and Pittman, 2005; Evert et al., 2006; McCampbell et al., 2000; Mueller et al., 2009; Shimohata et al., 2000). However, the expanded polyQ stretch in the C-terminus of ataxin-3 most likely leads to changes in protein conformation and binding properties in the disease. Moreover, losing protein function and altering subcellular localization were also observed in the disease (Macedo-Ribeiro et al., 2009). For example, mutant ataxin-3 showed a widespread reduction of protein deubiquitination in a cell model (Winborn et al., 2008). The reduction of deubiquitination function in MJD might be due to the aggregations of mutant ataxin-3 (Chai et al., 1999). Not only ubiquitin-proteasome degradation but also autophagic activation is altered in MJD. The aggregations of mutant ataxin-3 were observed in autophagosome and the stimulation of autophagy was found to alleviate aggregations and disease symptoms *in vivo* (Ravikumar et al., 2004). Moreover, it has been shown that mutant ataxin-3 induced oxidative stress could lead to mitochondrial dysfunction and cell damage (Laco et al., 2012). Another study also showed that overexpressing mutant

ataxin-3 in a cell model reduced antioxidant enzyme levels and increased

mitochondrial DNA damage, which indicated the mitochondrial function

was impaired in MJD (Yu et al., 2009). In addition, the mitochondrial

DNA copy numbers in MJD mice were far less than normal mice,

implying that mitochondria DNA damage was due to oxidative stress

(Kazachkova et al., 2013).

Nuclear aggregation is the major hallmark in the MJD patients. The

intracellular aggregations composed of expanded polyQ fragments and

full-length ataxin-3, were observed in cerebellar neurons and ventral pons

(Trottier et al., 1998). Moreover, the half-life of mutant ataxin-3 seemed

to be longer than normal ataxin-3 (Matsumoto et al., 2004), indicating

that blocked degradation by the ubiquitin proteasome pathway facilitates

mutant ataxin-3 aggregation. Therefore, "toxic fragment hypothesis" was

proposed to illustrate the proteolytic cleavage of mutant ataxin-3 in MJD

disorder pathogenesis (Berke et al., 2004; Haacke et al., 2006; Takahashi

et al., 2008). Additionally, mutant ataxin-3 was also found to be cleaved

by calpains and resulted in the formation of C-terminal ataxin-3

fragments for aggregation (Earnshaw et al., 1999). Calpain is a cysteine

protease activated by calcium. Several caspases and calpains proteolytic

enzymes were identified to be responsible for the generation of the toxic ataxin-3 fragments (Hubener et al., 2013). Inhibition of calpain resulted in reduced mutant ataxin-3 proteolysis, nuclear localization, aggregation and alleviated toxicity *in vitro* and *in vivo* (Haacke et al., 2007; Simoes et al., 2012). In addition, mutant ataxin-3 was found to bind to inositol 1,4,5-trisphosphate receptor type 1 (IP_3R1) and activate intracellular calcium release (Chen et al., 2008). Taken together, these findings suggest that altering cellular calcium homeostasis plays an important role in the pathogenesis of MJD.

Molecular analysis has shown that MJD is caused by a pathological expansion of a CAG repeat in exon 10 of the MJD1 gene. A MJD transgenic mouse (Tg) model was previously established by Cemal and colleagues (Cemal et al., 2002). The MJD Tg mice harbor two copies of human *ATXN3* gene with 84 CAG repeats. The Tg mice with expanded alleles demonstrated a mild and slowly progressive cerebellar deficit. As the disease progressed, the mice emerged hypotonia, motor and sensory loss. Neuronal intranuclear inclusion (NII) formation and neuronal cell loss were prominent in the pontine and in the cerebellum (Cemal et al., 2002).

1.2 Carbonic anhydrase 8 (CA8)

Carbonic anhydrase 8 (CA8) is a member of α-carbonic anhydrase family, which consists of 16 isozymes. Thirteen of the isozymes (CA1, 2, 3, 4, 5A, 5B, 6, 7, 9, 12, 13, 14 and 15) can catalyze the reversible hydration of carbon dioxide (CO_2) to bicarbonate and protons to maintain pH balance in blood (Berthelsen, 1982). There are three additional CA isozymes carbonic anhydrase related protein 8, 10, and 11(CA8, 10 and11), which do not have the activity due to lack one or more histidine residues that are required to catalyze CO_2 hydration (Picaud et al., 2009; Sjoblom et al., 1996). It is known that CA8 is predominantly present in the Purkinje cell layer of the cerebellum in mouse and human (Aspatwar et al., 2010; Hirota et al., 2003). The expression of CA8 is also observed in various organs, such as liver and lung (Hirota et al., 2003). Moreover, CA8 binds to inositol 1,4,5-trisphosphate receptor type 1 (IP_3R1) and decreases the affinity of IP_3 to the receptor (Hirota et al., 2003).

Previous studies of CA8 mainly focused on the roles of CA8 in neurodegeneration. It was reported that the *waddles* (*wdl*) mouse, exhibiting ataxic movement and dystonia, harbors a 19-bp deletion in ca8 gene (Jiao et al., 2005). Furthermore, two homozygous point mutations in

CA8 gene, S100P and G162R, were reported in patients with cerebellar ataxia and cerebellar atrophy in Iraqi families (Kaya et al., 2011; Turkmen et al., 2009). Recent studies from our laboratory also demonstrated that knockdown of CA8 in zebrafish larvae resulted in abnormal phenotypes, defective locomotion and neuronal cell death (Huang et al., 2014). In addition, we showed a significant decrease of CA8 mRNA and protein expression in cybrid cells containing MERRF A8344G mutation. Myoclonus epilepsy associated with ragged-red fibers (MERRF) syndrome is a mitochondrial disease with pathological features of ataxia and myoclonus. Moreover, overexpression of CA8 has been identified to play an protective function in MERRF cybrid cells (Wang et al., 2014). These findings support that CA8 plays an important role in neuron function and cerebellum development. Additionally, our previous results have revealed that CA8 was significantly increased in human neuroblastoma cells harboring mutant ataxin-3 as compared with cells containing normal ataxin-3 (Hsieh et al., 2013). However, the mechanisms underlying these observations remain to be addressed.

In this study, we hope to correlate the expression of CA8 with mutant

ataxin-3 in MJD cellular and animal models. MJD Tg mice and the wild type control, originally purchased from Jackson's lab, were kindly provided by Dr. Chin-San Liu at Changhua Christian Hospital. Together with two cellular models created in our laboratory, we aimed to understand the regulation and function of CA8 in the presence of mutant ataxin-3 *in vitro* and *in vivo*.

Materials and Methods

2.1 Cell lines and antibodies

Human neuroblastoma cell line SK-N-SH (HTB-11; ATCC) was provided by Dr. Shin-Lan Hsu (Taichung Veterans General Hospital, Taiwan) and human embryonic kidney cell line HEK293 (CRL-1573; ATCC) was provided by Dr. His-Chi Lu (Tunghai University, Taiwan). All materials for cell culture were obtained from Gibco Life Technologies (Gaithersburg, MD). Mouse monoclonal antibody against ataxin-3 was from Merck Millipore (Billerica, MA, USA). Rabbit polyclonal antibody against IP$_3$R1 was from Merck Millipore (Billerica, MA, USA). Mouse monocolyconal antibodies against HA and GFP were obtained from Santa Cruz Biotechnology (Santa Cruz, CA). Rabbit polycolyconal antibody against CA8 was obtained from Santa Cruz Biotechnology (Santa Cruz, CA). Mouse monoclonal antibodies against β-actin and α-tubulin were obtained from Novus Biologicals (Littleton, CO, USA).

2.2 Animals

C57BL/6J MJD mice expressing two copies of human ataxin-3 gene with

84 CAG repeats (Cemal et al., 2002) and their wild type littermates were provided by Dr. Chin-San Liu (Changhua Christian Hospital, Taiwan). Animals were maintained on a 12-h light/dark cycle with free access to food and water. All of the mouse-use protocols in this research were approved by the Institutional Animal Care and Use Committee of Tunghai University.

2.3 Isolation of total RNA and RT–PCR

Total RNA was extracted from the cerebellum of mice using TRIzol® reagent from Life Technologies. Semi-quantitative RT–PCR (reverse transcription PCR) was performed. Four µg of total RNA was reverse-transcribed into cDNA in a final volume of 20 µl with 50 pmol oligo-dT primer, 0.5 mM dNTP and 200 units of MMLV (Moloney murine leukaemia virus) reverse transcriptase (Life Technologies) for 50 min at 37°C and 15 min at 70°C. The primers used were: 5'-TCCTGATGCTAATGGGGAGTACCAG-3'and 5'-CTCAGGGG-CTG1GGTAGGTCGGAAA-3' for CA8, 5'-CCATGACAACTTTGGCA TTG-3' and 5'-CCTGCTTCACCACCTTCTTG-3'for GAPDH (Glyceraldehyde-3-phosphate-dehydrogenase). The PCR consisted of

varying cycles with denaturation at 94∘C for 30 s, annealing at 57∘C for

30 s, and elongation at 72°C for 30 s. The PCR-amplified DNA products

were electrophoretically separated on 1% agarose gels. In order to

compare the amplified products semi-quantitatively, signal quantification

was performed using a densitometric scanner (Image J). We confirmed

that the amounts of PCR products were at a linear range after 22 cycles of

PCR amplification.

2.4 Preparation of lysate for SDS/PAGE

The cerebellum tissues or cells were washed twice with PBS,

resuspended in 500 μl of lysis buffer (15% glycerol, 1 mM sodium EDTA,

1 mM sodium EGTA,1 mM DTT, 40 μg/ml leupeptin, 20 μg/ml pepstain,

1 mM PMSF and 0.5% Triton X-100 in PBS) and then sonicated on ice

for 15 min. The resulting lysate was centrifuged at 13000 rpm for 30 min

at 4°C. The supernatant was collected and the protein concentration was

determined by using the Bio-Rad protein assay.

2.5 Western blotting

The cell lysates containing 10-30 μg of protein were loaded by 10%

sodium dodecyl sulfate (SDS) polyacrylamide gels. The resolved proteins were electrophoretically transferred on to 0.2 μm PVDF membranes. After blocking the membrane with 5% (w/v) non-fat milk powder in TTBS (10 mM Tris/HCl (pH 7.5), 150 mM NaCl and 0.1% Tween 20) buffer for 1 hour at room temperature, the antibody-binding reaction was performed in the same buffer at 4°C overnight or at room temperature for 1 hour for primary antibodies and at room temperature for 1 hour for secondary antibodies to couple to HRP (horseradish peroxidase)-conjugated anti-(goat IgG) antibody. Pre-stained high-molecular-mass markers were included. Signals were captured by the enhanced chemiluminescent (Millipore). Protein bands were quantified by densitometry, and protein loading was normalized with β-actin or α-tubulin. For quantification of proteins, the amount of proteins loaded on to the gel was optimized, and multiple exposures were performed to ensure that the signals were within the linear response range.

2.6 Plasmid construction

Plasmid MJD26-GFP containing full-length MJD with 26 glutamines,

plasmid MJD78-GFP containing full-length MJD with 78 glutamines and plasmid tMJD78-GFP lacking N-terminus of MJD (with amino acids 20–244 deletion) were constructed by Wei-Hsiu Chang (Chang et al., 2009). pCDNA3.1 containing full-length MJD with 78 glutamines was a gift from Dr. Henry Paulson. A lentivirus transfer vector containing full-length CA8 with myc tagged (pLKOAS3w.puro.CA8-myc) was constructed by Tang-Hao Chi (unpublished data). The recombinant DNA sequence was confirmed by DNA sequencing. The lentiviral eGFP expression vectors of control (pLKOAS7w.eGFP.puro), shRNA expression vectors of sh-Ctrl (pLKO.1-shLuc) and sh-CA8 (TRCN000155916) were purchased from the National RNAi Core Facility (Institute of Molecular Biology, Academia Sinica, Taipei, Taiwan).

2.7 Cell culture and selection of stable cells

Human neuroblastoma cell line was maintained in a medium containing Dulbecco's modified Eagle's medium (DMEM) supplemented with 1% non-essential amino acid, 100 units/ml penicillin, 100 μg/ml streptomycin, 2 mM L-glutamine, 10% fetal bovine serum (FBS) and 100 μg/ml

pyruvate. SK-N-SH cells were transfected with pCDNA3-HAMJD78 and a stable cell line (SK-MJD78) was selected in culture medium supplemented with G418 (neomycin sulfate, 500 µg/ml) (Wen et al., 2003). Viruses carrying recombinant pLKOAS3w-CA8-myc.puro and pLKOAS7w.eGFP.puro were generated by the National RNAi Core Facility in Academia Sinica. Infection of the modified virus for stable expression of CA8 was performed according to the instructions provided by the National RNAi Core Facility. SK-MJD78 cells infected with recombinant lentivirus were selected using 0.7 µg/ml puromycin (Sigma). Expression of CA8 proteins was determined by Western blot analysis using an anti-CA8 antibody. Expression of eGFP proteins was determined by Western blot analysis using an anti-GFP antibody. After 5 days of selection, the surviving cells were grown in a medium 0.7 µg/ml of puromycin. Stable cells were collected after 10–15 days. Human embryonic kidney cell line was maintained in a medium (MEM) supplemented with 1% non-essential amino acid, 100 units/ml penicillin, 100 µg/ml streptomycin, 2 mM L-glutamine, 10% fetal bovine serum (FBS) and 100 µg/ml pyruvate. Cells were transfected using Polyjet reagent (SignaGen) following the manufacturer's instructions. Cells were

transfected with 1 µg of MJD26-eGFP, MJD78-eGFP or tMJD78-GFP. Eighteen hours after transfection, cells were selected in a culture medium supplemented with 500 µg/ml G418 (Life Technologies). Expression of GFP proteins was determined by Western blot analysis using an anti-GFP antibody. After 14 days of selection, the surviving cells were diluted to a density of 10 cells/ml and grown in a medium containing 500 µg/ml of G418. Stable cells were collected after 14–20 days. For all experiments, cells were placed in a medium lacking puromycin and G418.

2.8 Luciferase activity

A luciferase reporter plasmid containing the full-length of CA8 promoter was constructed by Cher-Min Lo (Lo et al., unpublished data). The construct was co-transfected into HEK293 cell lines (HEK293-MJD26, HEK293-MJD78 and HEK293-tMJD78) along with a β-galactosidase (β-gal) vector. After 48 h, luciferase activity was measured and normalized to β-galactosidase levels. Promoter activity was determined by measuring relative luciferase activity in the transfected cells using a luciferase reporter kit (Promega, Madison, WI). In these experiments, all the data were normalized to β-galactosidase activity.

2.9 Immunohistochemistry

The cerebellum tissues were isolated from mice at different ages and fixed at 4 ℃ in 4% paraformaldehyde (PA) in PBS overnight. The fixed cerebellum tissues were washed with PBS, and incubated in 10% sucrose solution at 4℃ for 1 h, in 20% sucrose solution at 4℃ for 2 h and in 30% sucrose solution at 4℃ overnight. The cerebellum tissues were frozen by OCT compound (Tissue Freezing Medium) and 10 μm sections were cut using a cryostat (LEICA CM3050S) at -20 ℃. After washing with PBS, cerebellum tissues were blocked using 10% fetal bovine serum (FBS) in PBS for 1 hour at room temperature. The samples were incubated with the primary antibody solution at 4 ℃ overnight (1:200 anti-CA8). Endogenous peroxidases were blocked using 30% hydrogen peroxide (H_2O_2) for 30 min at room temperature. After washing with PBS for 3 times, the samples were incubated with secondary antibodies for 2 h at room temperature (1:200 dilution, HRP conjugated goat anti-rabbit IgG). After washing with PBS, the diaminobenzidine substrate (DAB; KOMA) was added, and the reaction was stopped in PBS after the desired degree of straining was reached. Slides were counterstained with hematoxylin (Merck). Finally, slides were mounted by permount mounting medium

(Fisher Scientific). The immunohistochemistry results were scored by taking into account the intensity of the staining. Each slide was examined and scored blindly by 15 examiners who assigned a score of 0 (no staining), 1 (slightly staining), 2 (moderately staining), or 3 (most intense staining) within Purkinje cell layers.

2.10 Immunofluorescence

Cells were seeded on glass coverslips at 3×10^5 cells/well in 6-well tissue culture plates and incubated for 48 h at a $37^{\circ}C$ in a 5% CO2 incubator. The tissues were cut at 10 μm sections by a cryostat (LEICA CM3050S) at -20 ℃. Cells were then washed three times with PBS (pH 7.4), fixed and permeabilized with 4% paraformaldehyde (PA) in PBS for 20 min at room temperature. After washing with PBS, cells and tissues were blocked using 10% fetal bovine serum (FBS) in PBS for 1 h at room temperature. The samples were incubated with the primary antibody solution at 4 ℃ overnight (anti-ATXN3, 1:1000, 1:200 anti-CA8, 1:100 anti-GFP, 1:200 anti-HA and 1:100 anti-myc). After washing with PBS for 3 times, the samples were incubated with secondary antibodies and 3,8-Diamino-5-[3-(diethylmethylammonio)propyl]-6-phenylphenanthridi

nium diiodide (PI) for 2 h at room temperature (1:500 PI, 1:200 anti-mouse IgG FITC and anti-rabbit-IgG DyLight 649). Finally, cells and tissues were washed three times and mounted. The images were recorded on Zeiss LSM 510 confocal microscope.

2.11 Immunoprecipitation

Cells were solubilized in lysis buffer (50 mM Tris-Hcl, pH 7.9, 150 mM NaCl, 1% NP-40, 1X protein inhibitor cocktail, 10% glycerol, 1.5 Mm $MgCl_2$, 1mM EGTA, 1mM EDTA) and lysates were cleared by centrifugation. Equal amounts of total proteins were incubated with monoclonal anti-myc or polyclonal anti-CA8 for 1 h, and then incubated with A-Agarose beads overnight. The beads were pelleted by centrifugation and washed with washing buffer (50 mM Tris-Hcl, pH 7.9, 150 mM NaCl, 1% NP-40, 10% glycerol, 1.5 Mm $MgCl_2$, 1mM EGTA, 1mM EDTA). The immunopellets were resuspended in SDS-PAGE sample buffer and subjected to electrophoresis and Western blot analysis.

2.12 Mouse cerebellar granule neuron (CGNs) isolation and treatment

C57BL/6J WT and MJD mice (postnatal day 5–7) were anesthetized on ice for a few minutes before decapitation, then the crumbed meninges and cerebellum tissue were carefully removed using fine tweezers. The cerebellum tissue was then incubated for 10 min in 1 ml of dissociation solution containing 0.25% trypsin and 1 mM EDTA at 37 ℃, pipetted with P1000 pipet every 5 min, centrifuged at 1000 rpm for 5 min, and then the supernatant was removed. 10 μl of 10 mg/ml DNase I (Sigma) was added to the pellet, after briefly tipping the tube, 1 ml of DMEM containing 20% FBS was added into the tube. The mixture was centrifuged at 1000 rpm for 5 min, and then the supernatant was removed. Four ml of 20% FBS DMEM was added in to the pellet (cerebellar granule neurons). After cell counting, we seeded 1×10^6 CGNs into 3 cm dishes for the following experiments. For lentivirus infection, 5×10^5 of CGNs were seeded in 3 cm dishes with 20% FBS DMEM for 24 h. One day after, culture media were replaced by 20% FBS DMEM containing 8 μg/ml polybrene. According to the virus titer, we added the appropriate amounts of lentivirus carrying recombinant pLKOAS3w-CA8-myc-puro, CA8 shRNA (pLKO.1-shCA8, TRCN000155916), or control vector (pLKOAS7w.eGFP.puro and pLKO.1-shLuc) (M.O.I = 3) into CGNs for

12 h infection. After lentivirus infection, the infection medium was replaced by 20% FBS DMEM, selected by 1 µg/ml puromycin (Sigma) for 3 days and then incubated until cells were placed in a medium lacking puromycin before the experiments.

2.13 Cell viability

SK-N-SH cell lines were seeded at the density of 1.3×10^5 cells/well and CGNs were seeded at the density of 2×10^4 cells/well in a 96-well tissue culture plate incubated for 24 h in a 37 °C, 5% CO2 incubator. One day after seeding, cells were changed to medium and added H_2O_2 (20 µM and 3µM) for 30 min to SK-N-SH cell lines or CGNs. A23187 and calpeptin were added from stock solutions in dimethyl sulfoxide. Final concentration of dimethyl sulfoxide never exceeded 0.5%, and this concentration had no effect on cell viability. For treatments with various agents, culture plates containing A23187 (5 µM and 10 µM), calpeptin (20 µM and 10 µM) and BAPTA-AM (10µM and 5 µM) were treated for 10 min, 2 h and 30 min to SK-N-SH cell lines or CGNs, respectively, before treated with H_2O_2. Cell viability was determined with the 3-(4,5-dimethylthiazol-2-yl)-2,5-diphenyltetrazolium bromide (MTT)

assay (Sigma). Then MTT (5 mg/mL) were added to each well and the mixture was incubated at 37 ℃ for 4 h. To dissolve formazan crystals, culture medium was then replaced with an equal volume of DMSO. After the mixture was shaken at room temperature (RT) for 10 min, absorbance of each well was determined at 570 nm using a microplate reader. Results were expressed as the percentage of controls.

2.14 Measurement of intracellular Ca^{2+}

SK-N-SH cell lines were seeded at the density of 1.3×10^5 cells/well and mouse CGNs were seeded at the density of 2×10^4 cells/well in a 96-well tissue culture plate incubated for 24 h in a 37 ℃, 5% CO_2 incubator. After 24 h, cells were washed by HEPES buffer with Ca^{2+}, and loaded with 2.5 μM Fura-4AM in the HEPES buffer with Ca^{2+}. After 45 min, cells were washed by the HEPES buffer without Ca^{2+}, and incubated for 30 min. Finally, cytosolic Ca^{2+} signal in cells was assessed in response to 0.1mMATP. Fura-4AM fluorescence was recorded continuously at 37 ℃ in a spectrofluorometer at the excitation wavelength of 494 nm and an emission wavelength of 516 nm.

2.15 Measurement of 2-NBDG uptake

SK-N-SH cells were seeded at the density of 1.3×10^5 cells/well and CGNs were seeded at the density of 2×10^4 cells/well in a 96-well tissue culture plate incubated for 24 h in a 37 ℃, 5% CO2 incubator. After 3 h incubation in a medium with no glucose, cells were incubated with a fresh DMEM medium supplemented with 300 μM 2-(N-(7-Nitrobenz-2-oxa-1,3-diazol-4-yl)Amino)-2-Deoxyglucose (2NBDG) (Life technologies) for 1 h. After three times washed by PBS, 2NBDG fluorescence was recorded continuously at 37 ℃ in a spectrofluorometer at the excitation wavelength of 465 nm and an emission wavelength of 540 nm.

2.16 Statistics

Data are expressed as the mean ± standard error. The differences between groups were analyzed using the Student's t-test or Kruskal-Wallis test of variance. The difference was considered significant if the p value was less than 0.05.

Results

3.1 Protein expression of CA8 in a MJD Tg mouse model

We have previously demonstrated that the CA8 expression in mRNA and protein levels was higher in human neuroblastoma cells containing mutant ataxin-3 than that in control human neuroblastoma cells containing normal ataxin-3 (Hsieh et al., 2013). Therefore, we were interested in evaluating the expression levels of CA8 in the cerebellum tissue of MJD Tg mice. RT-PCR and Western blot analysis were performed to determine the CA8 expression levels and our results showed higher expression of CA8 in MJD Tg mice (Fig.1), as compared with the wild type (WT) control. In addition, the expression of mRNA and protein levels in Tg mice at age of 3 weeks or 52 weeks were both higher than those of the WT mice.

3.2 Immunohistochemistry of CA8 expression in WT and MJD Tg mice

A previously study has shown that the CA8 is predominantly present in the Purkinje cell layer of mouse cerebellum (Aspatwar et al., 2010). To

further confirm the increased expression of CA8 in MJD Tg mouse, we used immunohistochemical staining to examine the expression patterns of CA8. As shown in Figure 2, CA8 was detected in Purkinje cells and the more intense staining was observed in MJD Tg mouse of 3 weeks and 52 weeks, as compared with the control WT mouse. To quantify the results, a scoring system by taking into account the intensity of staining (Tsai et al., 2014) was used for immunohistochemical staining. Quantitative analysis demonstrated that a significant increase of CA8 was observed in MJD Tg mice of 3 weeks, 26 weeks and 52 weeks of age compared with those in WT mice (Fig. 2E). It is worth noting that as the mice became aged, the expression level of CA8 was gradually decreased in MJD Tg mice.

3.3 Increased CA8 promoter activity in HEK293-MJD78 cells

To establish a set of MJD disease cellular model, we transfected three constructs containing normal ataxin-3 (MJD26), mutant ataxin-3 (MJD78) and N-terminal truncated mutant ataxin-3 (tMJD78) into human embryonic kidney cells (Chang et al., 2009) (Fig.3A). Stable clones designated HEK293-MJD26, HEK293-MJD78, and HEK293-tMJD78 were

established by proper antibiotic selection. As shown in Figure 3B, the expression of ataxin-3 was confirmed in all three stable cell lines. Consistent with what observed in SK-MJD78-CA8 cells, the expression of CA8 showed increased in HEK293 cells containing mutant ataxin-3, as compared with that in cells harboring normal ataxin-3.

Because the increased protein and mRNA levels of CA8 may indicate altered transcription regulation, we assayed the promoter activity of CA8 in HEK293 stable cells with normal or mutant ataxin-3. We transfected a luciferase reporter plasmid containing the full-length of CA8 promoter (Lo et al., unpublished data) into HEK293 cell lines harboring normal ataxin-3, mutant ataxin-3 and truncated mutant ataxin-3 (HEK293-MJD26, HEK293-MJD78 and HEK293-tMJD78) along with a β-gal vector as a tranfection control. As shown in Figure 3C, the luciferase activity of HEK293-MJD78 cells was clearly higher than that of HEK293-MJD26 cells, suggesting that CA8 may be up-regulated in the transcription level in the presence of mutant ataxin-3.

3.4 CA8 is co-localized with mutant ataxin-3 in SK-MJD78-CA8 and in HEK293-MJD78 cells

Our previous study demonstrated that the mRNA expression of CA8 in SK-MJD78 cells was more than that in SK-MJD26 cells (Hsieh et al., 2013). However, due to the lack of endogenous CA8 protein detected by commercial antibody in SK-MJD78 cells (Fig.4), viruses carrying recombinant plasmid pLKOAS3w.puro.CA8-myc (a lentivirus transfer vector containing full-length CA8) and pLKOAS7w.eGFP.puro (control virus) were used to infect SK-MJD78 cells. Stable clones, designated SK-MJD78-eGFP (SK-MJD78 cells infected with virus carrying pLKOAS7w.eGFP.puro) and SK-MJD78-CA8 (SK-MJD78 cells infected with virus carrying pLKOAS3w.puro.CA8-myc), were obtained after proper antibiotic selection. As shown in Figure 4, the ectopic expression of CA8 was confirmed in SK-MJD78-CA8 cells, with a positive control signal of CA8 from HOS-CA8 cells (Fig. 4A). In addition, GFP expression was clearly detected in SK-MJD78-eGFP with HOS-eGFP as a positive control (Fig. 4B). Normal and mutant ataxin-3 expression was also validated in those four cell lines (Fig. 4C). Next, we examined the distributions of ataxin-3 and CA8 in SK-MJD78 cells with stably

overexpressed CA8 (SK-MJD78-CA8) or in HEK293 cells with stably overexpressed normal full-length ataxin-3 (HEK293-MJD26), mutant full-length ataxin-3 (HEK293-MJD78), or mutant truncated ataxin-3 (HEK293-tMJD78) by immunofluorescence. As shown in Figure 5A, both CA8 and mutant ataxin-3 were mainly distributed in the cytoplasm and co-localized together. Consistently, the results from immunofluorescence also showed the same distribution and co-localization of CA8 and mutant ataxin-3 in HEK293-MJD78 cells (Fig. 5B). It is noted that there was no difference in the distribution of CA8 among those three HEK293 cell lines, suggesting that the cellular distribution of CA8 is not altered by the presence or absence of mutant ataxin-3.

3.5 CA8 interacts with mutant ataxin-3 in MJD disease cellular model

It is known that mutant ataxin-3 interacts with inositol 1,4,5-trisphosphate receptor type 1 (IP$_3$R1) (Chen et al., 2008). In addition, CA8 interacts with IP$_3$R1 and acts as an IP$_3$R1-binding protein (Hirota et al., 2003).

Because our results showed that CA8 and ataxin-3 were co-localized in SK-MJD78-CA8 and HEK293 cell lines. We next tried to examine the possible interaction between CA8 and ataxin-3 in SK-MJD78-CA8 and HEK293 cell lines by immunoprecipitation. Interestingly, our analysis revealed a protein-protein interaction between CA8 and ataxin-3 in SK-MJD78-CA8 cells (Fig. 6A and 6B). Moreover, our results showed that the interaction existed only between CA8 and mutant ataxin-3 in HEK293-MJD78 cells but not in HEK293-MJD26 or HEK293-tMJD78 cells (Fig. 6D). Meanwhile, we also tried to determine whether the endogenous CA8 interacts with mutant ataxin-3 by using cerebellum extract from MJD Tg mice. Unfortunately, we failed to detect the interaction between CA8 and ataxin-3 using antibody against CA8 (Fig.7A and 7B). Given the fact that the interaction of mouse endogenous CA8 and mutant ataxin-3 cannot be revealed by immunoprecipitation, we examined the distribution of CA8 and mutant ataxin-3 in MJD Tg mouse cerebellum by immunofluorescence. As shown in Figure 7C, CA8 and mutant ataxin-3 were co-located in Purkinje cells of MJD Tg mice. The results suggest that the interaction between endogenous CA8 and mutant ataxin-3 in MJD Tg mice may be relatively weak and cannot be observed

by the current experimental condition.

3.6 Overexpression of CA8 decreases cell death upon H$_2$O$_2$ treatment

We have previously shown that neuroblastoma cells containing mutant ataxin-3, SK-MJD78 cells, are more susceptible to oxidative stress than the control cells by MTS assay (Wen et al., 2003). It is noted that overexpression of CA8 in MERFF mutant cells protected cells from apoptosis upon pro-apoptotic treatment (Wang et al., 2014). Therefore, we aimed to understand whether CA8 plays protective effects on SK-MJD78 cells by using cell survival assay. Briefly, cells were treated with 20 μM H$_2$O$_2$ for 30 min and then MTT assay was performed in a spectrofluorometer at excitation wavelength of 570 nm. As shown in Figure 8A, SK-MJD78 cells were more susceptible to oxidative stress than the parental SK-N-SH cells, which is consistent with our previous report (Wen et al., 2003). Furthermore, overexpression of CA8 desensitized cells to H$_2$O$_2$ treatment as compared with that in SK-MJG78-eGFP cells (Fig. 8B), supporting a protective role of CA8 in the MJD disease cellular model.

Given the results that overexpression of CA8 prevented cell death in

cellular models, it is possible that the protective effect of CA8 is also true in MJD cerebellar granule neurons (CGNs). To examine the effects of CA8 on granule neuron survival, CGNs were isolated from WT and MJD Tg mice, and then infected with viruses carrying overexpressing CA8, CA8-shRNA and control pLKO.1-shLUC and pLKOAS7w.eGFP.puro, respectively. As shown in Figure 9A, the expression level of CA8 was significantly increased in CGNs with overexpressing CA8; moderately decreased in CGNs with the down-regulated of CA8, as compared with that of the individual control. To examine the effects of CA8, the infected CGNs were further treated with 3 μM H_2O_2 and cell viability was measured by MTT assay. The results showed no significant difference of cell viability between wild type CGNs overexpressing or down-regulated CA8 expression (Fig. 9B and C). However, overexpression of CA8 in MJD CGNs resulted in a significant increase of cell survival as compared with that of control cells (Fig. 9E). These findings suggest that up-regulation of CA8 has protective effects not only on neuronal cell lines but also on primary granule neurons from MJD Tg mice.

3.7 CA8 rescues abnormal Ca^{2+} release in SK-MJD78-CA8 cells and

in MJD CGNs

Previous evidence showed that neuronal Ca^{2+} signaling was abnormally increased in the pathogenesis of SCA3 (Bezprozvanny, 2009). Mutant ataxin-3 was also found to interact with IP_3R1 and activate the intracellular calcium release by an agonist of IP_3R1 (Chen et al., 2008). In addition, CA8 was proved to interact with IP_3R1 and regulate Ca^{2+} release via influencing IP_3 binding to its receptor IP_3R1 on the ER. Therefore, we aimed to examine whether any alteration of Ca^{2+} release exists in SK-N-SH cells with and without mutant ataxin-3 and whether CA8 overexpression influences Ca^{2+} signaling. We first measured the calcium release in SK-N-SH cells with or without mutant ataxin-3, as well as in SK-MJD78 cells with or without CA8 expression under a 0.1 mM ATP stimulus. To block Ca^{2+} influx due to the activity of the store-operated channel, the experiment was performed in the absence of extracellular Ca^{2+} ions. Based on our experimental conditions, the increase of cytosolic Ca^{2+} after the addition of ATP was largely from the ER pool. Our results demonstrated that ATP induced a transient elevation of Ca^{2+} for all tested cells. As shown in Figure 10A, cells containing mutant ataxin-3 (SK-MJD78) showed a significantly increased cytosolic Ca^{2+} signaling in

response to 0.1 mM ATP compared with that in the WT cells (SK-N-SH cells). As expected, overexpression of CA8 in SK-MJD78-CA8 cells significantly reduced abnormal cytosolic Ca^{2+} signaling as compared with that in SK-MJD78-eGFP cells (Fig. 10B).

Meanwhile, we also tried to determine whether overexpression of CA8 decreases cytosolic Ca^{2+} signaling in MJD CGNs. Interestingly, no significant difference of Ca^{2+} release was detected between WT CGNs infected with lentiviral CA8 and lentiviral eGFP (Fig. 11B). However, both wild type and MJD CGNs with down-regulated CA8 showed siginifcantly increased cytosolic Ca^{2+} signaling in response to 0.1mM ATP, as compared with the lentiviral-control infected neurons. (Fig. 11 A and C). In contrast, overexpression of CA8 in MJD CGNs significantly decreased abnormal calcium release as compared with that of the lentiviral-control infected neurons (Fig. 11D).

Our findings confirm the abnormal Ca^{2+} release in neuronal cells harboring mutant ataxin-3 and further demonstrate that overexpression of CA8 rescues the abnormal Ca^{2+} signaling due to the presence of mutant ataxin-3.

3.8 Calcium ionophore counteracts the protective effect of CA8 in SK-MJD78-CA8 cells and in MJD CGNs

To confirm the effects of CA8 on Ca^{2+}-induced cell survival, we treated cells with different agents that are known to influence the Ca^{2+} influx. Calcium ionophore A23187, a mobile ion-carrier that forms stable complexes with divalent cations (Pressman, 1976), is widely used to increase intracellular calcium levels. In order to correlate intracellular calcium concentration and cell survival in the cell model, we induced Ca^{2+} release and examined the cell survival of SK-N-SH cells in the presence or absence of mutant ataxin-3 and CA8. As shown in Figure 12A, the cell survival rate of SK-MJD78 cells treated with Ca^{2+} ionophore was significantly lower than that of SK-MJD78 cells treated with H_2O_2 only. Moreover, when SK-MJD78-CA8 cells were treated with calcium ionophore, a significant decrease of cell survival was observed, suggesting that calcium ionophore induced calcium release counteracted the protective effect of CA8 (Fig. 12B).

Meanwhile, to determine whether the same effect could be observed in CGNs, CGNs were used for calcium ionophore treatment. As shown in Figure 12D, the cell survival of MJD CGNs pre-treated with Ca^{2+}

ionophore was significantly decreased compared with MJD CGNs treated with H_2O_2 only. Moreover, when MJD CGNs with overexpressing CA8 were treated with calcium ionophore, cell survival was reduced to the level similar to that in MJD CGNs treated with H_2O_2 alone (Fig. 12F). Our results suggest that calcium ionophore treatment in either SK-MJD78-CA8 or MJD CGNs with overexpressing CA8 counteracted the protective effect of CA8.

3.9 CA8 shows no effects on cell survival of SK-MJD78 cells with calpeptin treatment

Calpain is one of cysteine proteases and is dependent on calcium to attain functionally active forms (Saez et al., 2006). It is known that altered calpain activity was associated to the cleavage of mutant ataxin-3 in MJD disease. Calpain inhibitors reduced mutant ataxin-3 proteolysis and prevented cell toxicity in MJD (Haacke et al., 2007). Calpeptin, an inhibitor of calpains, is a cell-permeable of calpain inhibitor (Wang, 1990). Thus, we wanted to determine whether a calpeptin pre-treatment may inhibit calpain activity and altered cell survival when cells were challenged with H_2O_2. As shown in Figure 13A, cell survival of the cells

pretreated with calpeptin was significantly higher than that in the cells treated with H_2O_2 only. Interestingly, the cell survival showed no difference in SK-MJD78-CA8 cells with or without calpeptin pre-treatment (Fig. 13B). Similarly, the survival MJD CGNs pretreated with calpeptin was significantly higher than that of MJD CGNs without calpeptin pre-treatment (Fig. 13C and D). However, calpeptin pre-treatment showed no effects on cell survival of MJD CGNs with overexpressing CA8 upon the treatment of H_2O_2 (Fig. 13F).

3.10 CA8 shows no effects on cell survival of SK-MJD78 cells and MJD CGNs with overexpressing CA8 under BAPTA-AM treatment

BAPTA-AM, (N,N'-[1,2-ethanediylbis (oxy-2,1-phenylene)] bis [N-[2-[(acetyloxy) methoxy]-2-oxoethyl]-1,1'-bis[(acetyloxy)methyl] ester-glycine), is membrane-impermeable calcium chelator that binds extracellular calcium ions. The presence of four carboxylic acid functional groups makes possible the binding of two calcium ions. It is known that BAPTA-AM blocks extracellular Ca^{2+}-induced intracellular Ca^{2+} increase (Lee et al., 2012). Thus, we want to determine whether BAPTA-AM pre-treatment may alter cell survival in cells with or without

CA8 expressing under H_2O_2 challenge. As shown in Figure 14A, the cell survival was significantly higher in SK-MJD78 cells pretreated with BAPTA-AM, compared to that in cells treated with H_2O_2 only. However, BAPTA-AM pre-treatment showed no effects on cell survival of SK-MJD78-CA8 cells upon H_2O_2 treatment (Fig. 14B). On the other hand, the cell survival of BAPTA-AM pretreated WT CGNs, with different expression levels of CA8, was significantly higher than that of CGNs without BAPTA-AM pre-treatment (Fig. 14C, D and E). However, it is worth noting that the cell survival showed no difference in CA8 overexpressing MJD CGNs with or without BAPTA-AM pre-treatment (Fig. 14F).

3.11 CA8 overexpression partially increases glucose uptake in SK-MJD78-CA8 cells

It is known that progressive weight loss is a common finding in MJD patients and HD patients (Soong et al., 1997), suggesting that there may be a metabolic defect involved in the polyglutamine diseases. In addition, lower body weight was reported in over 90% of MJD mice, indicating that it may be a high-penetrant trait (Cemal et al., 2002). Moreover, our

previous study of the effects of CA8 on osteosarcoma revealed that overexpression of CA8 may be involoved in glycolytic activation (Wang et al., unpublished data). Therefore, we used 2-[N-(7-nitrobenz-2-oxa-1,3-diazol-4-yl)amino]-2-Deoxyglucose (2-NBDG) to detect the glucose uptake in MJD cellular models. 2-NBDG is a fluorescent indicator for direct glucose uptake measurement (Zou et al., 2005). As shown in Figure 14, the glucose uptake of SK-N-SH cells was significantly higher than that of SK-MJD78 cells. CA8 overexpression in SK-MJD78-CA8 cells resulted in an increase of glucose uptake as compared with that in SK-MJD78-eGFP cells (control). Furthermore, the glucose uptake ability showed no significant difference in WT CGNs with down-regulated or overexpressing CA8 (Fig. 15B). However, the glucose uptake in MJD CGNs with overexpressing CA8 was significantly increased compared with that in the lentiviral-control infected neurons (Fig. 15C). These findings suggest that the glucose uptake ability is decreased in cells harboring mutant ataxin-3 and the reduced ability could be partially increased through overexpressing of CA8 in neuronal cells.

Discussion

We have previously demonstrated that mRNA and protein levels of CA8 are higher in human neuroblastoma cells harboring mutant ataxin-3 (Hsieh et al., 2013). In order to confirm the expression levels of CA8 in an animal model, we obtained MJD tg mice (Cemal et al., 2002) and WT mice for comparison. We found that the mRNA and protein levels of CA8 were significantly increased in MJD tg mice (Fig. 1). In addition, consistent with the previous study, the expression of CA8 was mainly distributed in Purkinje cells by immunohistochemistry. To assess the intensity in the immunohistochemical staining, a scoring system by taking into account the different staining intensity of the positive signals was used (Tsai et al., 2014)(Fig. S1). Our results again confirmed that CA8 was detected in Purkinje cells, with a more intense staining in MJD mice as compared to WT control (Fig. 2). Moreover, we showed significantly altered CA8 expression in the cerebellum of MJD mice in the age of 3 weeks, 26 weeks and 52 weeks, supporting that mutant ataxin-3 expression contributes to the increase of CA8 expression. Furthermore, we observed a gradual decrease of CA8 expression along with aging in

MJD tg mice only. To study the mechanism underlying the altered CA8 expression, we established three human embryonic kidney cell lines containing normal ataxin-3 (MJD26), mutant ataxin-3 (MJD78) and N-terminus truncated mutant ataxin-3 (tMJD78), for assaying transcription activity. To validate the ectopic ataxin-3 expression in three stable clones, western blot was performed first. As shown in Figure 3B, the expression of truncated ataxin-3 was not detected because ataxin-3 antibody was raised against region E214-L233 of the N-terminal Josephin domain, which was truncated from tMJD78. Therefore, the expression of truncated ataxin-3 was confirmed by tagged GFP antibody (Fig. 3B). To determine the transcription activity of CA8 gene in the three stable clones, transient transfection of luciferase reporter plasmid containing the full-length CA8 promoter was performed. As shown in Figure 3C, mutant ataxin-3 significantly increased the luciferase activity in HEK293MJD78 compared with that of HEK293MJD26 and HEK293tMJD78, indicating the upregulation of CA8 only in the present of mutant ataxin-3.

Our previous studies showed that transient expression of mutant ataxin-3 altered the expression of CA11 in SK-N-SH cells and CA11 was redistributed into the nuclei and aggregated in cells expressing truncated

ataxin-3 (Hsieh et al., 2013). In addition, it is noted that CA8 was located in the cytoplasm (Aspatwar et al., 2010). In this regard, whether CA8 is redistributed into the nuclei in the presence of mutant ataxin-3 remains to be addressed. To examine the cellular localization of CA8 and mutant ataxin-3, immunofluorescence was carried out. Our results showed that CA8 was mainly distributed in the cytoplasm and co-localized, at least partially, with normal, mutant or truncated ataxin-3 (Fig. 5), suggesting that the cellular localization of CA8 was not altered by mutant ataxin-3. In addition, immunoprecipitation revealed that CA8 interacted with mutant ataxin-3 in SK-MJD78-CA8 and HEK293-MJD78 cells (Fig. 6). However, we failed to confirm the interaction between endogenous CA8 and mutant ataxin-3 by using cerebellar tissue from MJD tg and wild type mice (Fig. 7A and B). However, immunofluorescence showed that mutant ataxin-3 and CA8 were co-localized in the Purkinje layer of mouse cerebellum (Fig. 7C). This discrepancy between cellular and animal models may be due to a very weak interaction between CA8 and mutant ataxin-3. In other words, we suspect that the amount of endogenous CA8 is not enough to bring down the weakly interacted mutant ataxin-3 in our experimental conditions.

We have previously shown that the neuroblastoma cells containing mutant ataxin-3, SK-MJD78, are more susceptible to oxidative stress than the control cells (Wen et al., 2003). Moreover, we reported a protective function of CA8 in cells harboring the A8344G mutation of mitrochondrial DNA (Wang et al., 2014) and CA8 knockdown also impaired brain development through increased neuronal cell death (Aspatwar et al., 2013). Therefore, we speculated that the proper expression of CA8 in SK-MJD78 cells may also play an important role in cell protection. To investigate the possible protective role of CA8, ROS stress was applied to SK-N-SH, SK-MJD78,SK-MJD78-eGFP and SK-MJD78-CA8 cells. As expected, overexpression of CA8 significantly increased the cell surivial of SK-MJD78-CA8 cells as compared with that of the control cells after H_2O_2 treatment (Fig. 8B). Interestingly, WT CGNs with overexpressing CA8 showed no altered cell survival as compared with that of the lentiviral-control infected neurons after H_2O_2 treatment (Fig. 9B and C). However, under H_2O_2 treatment, the cell survival of WT or MJD CGNs with down-regulated CA8 showed no significant decrease in WT or MJD CGNs infected with the lentiviral-control (Fig. 9B and D). It is noted the down-regulation of CA8

by lentiviral shCA8 only rescued cell revival to 50% and 43% of that in the WT or MJD CGNs, which may explain why MJD CGNs with down-regulated CA8 did not show significant alteration in the cell survival. Moreover, MJD CGNs with overexpressing CA8 significantly increased the cell survival as compared with that of the lentiviral-control infected neurons after H_2O_2 treatment (Fig. 9E), further supporting a general protective role of CA8 in human neuronal cells and in MJD CGNs.

Recent evidence showed that abnormal neuronal Ca^{2+} signaling plays an important role in the pathogenesis of SCA3 (Bezprozvanny, 2009). It is known that CA8 interacts with IP_3R1 and suppresses the binding affinity of IP_3 to the receptor IP_3R1 (Hirota et al., 2003). Moreover, mutant ataxin-3 interacts with IP_3R1 and activates the intracellular calcium release by an agonist of IP_3R1 (Chen et al., 2008). Given the fact that down-regulation of CA8 in cybrids resulted in a significant increase of ATP-induced Ca^{2+} release (Wang et al., 2014), we attempted to detect the effect of CA8 on Ca^{2+} signaling in MJD cellular and animal models. Our results showed a significant decrease of calcium release in SK-MJD78-CA8 cells as compared with SK-MJD78-eGFP cells (Fig.

10B). Similarly, our results showed a significant decrease of calcium release in MJD CGNs with overexpressing CA8 as compared with the lentiviral-control infected neurons (Fig. 11D). It is worth noting that there was no difference of caiclum release between WT CGNs with overexpressing CA8 and the lentiviral-control (Fig. 11B). Interestingly, both WT CGNs and MJD CGNs with down-regulated CA8 show a significant increase of Ca^{2+} signaling compared with that in control WT and MJD CGNs (Fig. 11A and C). Even though the reduction of CA8 was only less than 50% in shRNA treated CGNs, it still caused the abnormal Ca^{2+} release. However, the abnormal Ca^{2+} release did not directly correlate to a similar effect on cell death, suggesting that the abnormal Ca^{2+} release was one of the reasons triggering the cell death. Taken together, our observation support the notion that overexpression of CA8 is critical in the modulation of intracellular Ca^{2+} signaling, which may be responsible for the protective function in human neuroblastoma cells and in MJD CGNs.

In order to confirm the results that the Ca^{2+} release plays an important role in cell survival, we used two drugs to test our hypothesis. Calcium ionophore A23187 is commonly used to increase intracellular Ca^{2+} levels

in mammalian cells (Martina et al., 1994). To determine the effects of CA8, neuroblastoma cells and CGNs were treated with 5 μM A23187 to increase Ca^{2+} release and then cells were challenged with H_2O_2. Interestingly, the cell survival of SK-N-SH and WT CGNs under H_2O_2 treatment was not affected by the addition of calcium ionophore (Fig. 12A ,C and D). Nevertheless, the same concentration of A23187 treatment led to a significant decrease of cell survival in SK-MJD78 cells and in MJD CGNs (Fig. 12B, E and F). Moreover, the survival of SK-MJD78-CA8 or MJD CGNs with overexpressing CA8 showed a significant decrease under the Ca^{2+} ionophore treatment. Our results suggest that increased Ca^{2+} release might counteract the protective function of CA8 in cells harboring mutant ataxin-3.

On the other hand, calpeptin is an inhibitor of calpain. The activation of calpain has been shown to be responsible for mutant ataxin-3 cleavage in MJD disease (Haacke et al., 2006). It is known that calpain inhibitor treatment resulted in reduced mutant ataxin-3 proteolysis and prevented cell toxicity in neurodegenerative diseases model (Haacke et al., 2006; Haacke et al., 2007; Simoes et al., 2012). Therefore, we treated neuroblastoma cells and CGNs with calpeptin and assayed for the cell

survival under H_2O_2 challenge. As expected, SK-N-SH cells and WT CGNs pre-treated with calpeptin showed a significant increase of cell survival upon H_2O_2 challenge (Fig. 13A, C and D). Furthermore, the cell survival of SK-MJD78 cells and MJD CGNs also increased under calpeptin pre-treatment, indicating the calpeptin inhibited the function of calpain. However, SK-MJD78-CA8 cells and MJD CGNs with overexpressing CA8 did not show a significant alteration of cell survival after calpeptin treatment (Fig. 13B and F). It is worth noting that calpains are activated by calcium and cause cell death (Simoes et al., 2012). Considering, overexpression of mutant atxin-3 in SK-MJD78 cells and MJD CGNs caused more abnormal Ca^{2+} release (Fig.10A and S2), the abnormal Ca^{2+} release may contribute to calpain activation and lead to cell death. Thus, SK-N-SH cells and mouse CGNs treated with calpeptin may lead to decreased cell death via inhibiting calpain activity. However, because overexpression of CA8 in SK-MJD78-CA8 cells and in MJD CGNs decreased the abnormal Ca^{2+} release, we speculated that the reduced caicium release may result in less activated calpains. Therefore, SK-MJD78-CA8 cells and MJD CGNs with overexpression of CA8 did not show any increase of cell survival under the calpeptin treatment.

BAPTA-AM is a well-known membrane permeable Ca^{2+} chelator and it can be used to control the level of intracellular Ca^{2+} (Ricci et al., 1998). Hence, we tried to determine whether BAPTA-AM pre-treatment may decrease Ca^{2+} and altered cell survival in the MJD disease cellular model. We treated neuroblastoma cells and CGNs with BAPTA-AM and assayed for the cell survival under H_2O_2 challenge. As shown in Figure 14, WT CGNs pre-treated with BAPTA-AM showed a significant increase of cell survival upon H_2O_2 challenge. Furthermore, the cell survival of SK-MJD78 cells and MJD CGNs also increased under BAPTA-AM treatment, indicating BAPTA-AM decrease Ca^{2+} release and reduce cell death in SK-MJD78 cells and MJD CGNs (Fig. 14B and F). However, SK-MJD78-CA8 cells and MJD CGNs with overexpressing CA8 did not show any alteration on cell survival after BAPTA-AM treatment, suggesting that in cells haboring mutant ataxin3, CA8 fails to further reduce calcium release in the presence of calcium chelator (Fig. 14B and F). Taken together, our results support and extend the notion that CA8 has a potential function to rescue abnormal Ca^{2+} release and decrease cell death in MJD cellular and animal models.

On the other hand, it is noted that progressive weight loss is a common

finding in MJD patients and MJD tg mice. Lower body weight was also reported in over 90% of MJD tg mice, suggesting that a metabolic defect may be involved in the diseases pathogenesis (Cemal et al., 2002). Recently, we found that CA8 may be able to influence the glucose uptake of HOS cancer cells (Wang et al., unpublished data). Therefore, we further investigated the effects of CA8 on glucose uptake ability in this disease model. Our results of glucose uptake assays showed no difference between WT granule neurons with down-regulationed CA8 and WT CGNs with overexpressing CA8 (Fig. 15B). However, the glucose uptake of SK-MJD78 cells and MJD CGNs were significantly decreased as compard with that of SK-N-SH and WT CGNs, respectively (Fig. 15A and C). In contrast, an increased glucose uptake was observed in SK-MJD78-CA8 cells and in MJD CGNs with overexpressing CA8 as compared with SK-MJD78 cells and the lentiviral-control infected CGNs (Fig. 15A and C). Our results suggest that mutant ataxin-3 may reduce the glucose uptake and subsequently affect the metabolic function; overexpression of CA8 may partially rescue the glucose uptake defect in SK-MJD78 cells and in MJD CGNs. However, more investigations will be needed to reveal the underlying mechanisms of the altered glucose

metabolism invloved in MJD.

In summary, our results revealed several important findings in Machado-Joseph disease. We demonstrate a significant increased expression of CA8 in MJD cerebellar tissues. The immunostaining of CA8 in MJD tg mice was found to be dynamic and gradually decreased with age. In addition, overexpression of CA8 desensitizes SK-MJD78 cells and MJD CGNs to H_2O_2 treatment, supporting the protective role of CA8. Moreover, overexpression of CA8 in SK-MJD78-CA8 cells and in MJD CGNs results in a significant decrease in calcium release, indicating that the protective function may be via the reduced calcium signaling (Fig. 16). In the present study, we were the first to report the noval protective function of CA8 in the pathogenesis of MJD. We speculate that the increased expression of CA8 in the disease early stage but decreased later on may be related to the late onset phenomenon. Although the detailed underlying mechanism still needs further investigation, we hope that our findings may provide important information for potential therapeutic targets in the future.

References

Aspatwar, A., Tolvanen, M.E., Jokitalo, E., Parikka, M., Ortutay, C., Harjula, S.K., Ramet, M., Vihinen, M., and Parkkila, S. (2013). Abnormal cerebellar development and ataxia in CARP VIII morphant zebrafish. Human molecular genetics *22*, 417-432.

Aspatwar, A., Tolvanen, M.E., and Parkkila, S. (2010). Phylogeny and expression of carbonic anhydrase-related proteins. BMC molecular biology *11*, 25.

Berke, S.J., Schmied, F.A., Brunt, E.R., Ellerby, L.M., and Paulson, H.L. (2004). Caspase-mediated proteolysis of the polyglutamine disease protein ataxin-3. Journal of neurochemistry *89*, 908-918.

Berthelsen, P. (1982). Cardiovascular performance and oxyhemoglobin dissociation after acetazolamide in metabolic alkalosis. Intensive care medicine *8*, 269-274.
Bezprozvanny, I. (2009). Calcium signaling and neurodegenerative diseases. Trends in molecular medicine *15*, 89-100.

Burnett, B.G., and Pittman, R.N. (2005). The polyglutamine neurodegenerative protein ataxin 3 regulates aggresome formation. Proceedings of the National Academy of Sciences of the United States of America *102*, 4330-4335.

Cemal, C.K., Carroll, C.J., Lawrence, L., Lowrie, M.B., Ruddle, P., Al-Mahdawi, S., King, R.H., Pook, M.A., Huxley, C., and Chamberlain, S. (2002). YAC transgenic mice carrying pathological alleles of the MJD1 locus exhibit a mild and slowly progressive cerebellar deficit. Human molecular genetics *11*, 1075-1094.

Chai, Y., Koppenhafer, S.L., Shoesmith, S.J., Perez, M.K., and Paulson, H.L. (1999). Evidence for proteasome involvement in polyglutamine disease: localization to nuclear inclusions in SCA3/MJD and suppression of polyglutamine aggregation in vitro. Human molecular genetics *8*, 673-682.

Chai, Y., Shao, J., Miller, V.M., Williams, A., and Paulson, H.L. (2002). Live-cell imaging reveals divergent intracellular dynamics of polyglutamine disease proteins and supports a sequestration model of pathogenesis. Proceedings of the National Academy of Sciences of the United States of America *99*, 9310-9315.

Chang, W.H., Tien, C.L., Chen, T.J., Nukina, N., and Hsieh, M. (2009). Decreased

protein synthesis of Hsp27 associated with cellular toxicity in a cell model of Machado-Joseph disease. Neuroscience letters *454*, 152-156.

Chen, X., Tang, T.S., Tu, H., Nelson, O., Pook, M., Hammer, R., Nukina, N., and Bezprozvanny, I. (2008). Deranged calcium signaling and neurodegeneration in spinocerebellar ataxia type 3. The Journal of neuroscience : the official journal of the Society for Neuroscience *28*, 12713-12724.

Coutinho, P., and Andrade, C. (1978). Autosomal dominant system degeneration in Portuguese families of the Azores Islands. A new genetic disorder involving cerebellar, pyramidal, extrapyramidal and spinal cord motor functions. Neurology *28*, 703-709.

Durcan, T.M., and Fon, E.A. (2013). Ataxin-3 and its e3 partners: implications for machado-joseph disease. Frontiers in neurology *4*, 46.

Earnshaw, W.C., Martins, L.M., and Kaufmann, S.H. (1999). Mammalian caspases: structure, activation, substrates, and functions during apoptosis. Annual review of biochemistry *68*, 383-424.

Evers, M.M., Toonen, L.J., and van Roon-Mom, W.M. (2014). Ataxin-3 protein and RNA toxicity in spinocerebellar ataxia type 3: current insights and emerging therapeutic strategies. Molecular neurobiology *49*, 1513-1531.

Evert, B.O., Araujo, J., Vieira-Saecker, A.M., de Vos, R.A., Harendza, S., Klockgether, T., and Wullner, U. (2006). Ataxin-3 represses transcription via chromatin binding, interaction with histone deacetylase 3, and histone deacetylation. The Journal of neuroscience : the official journal of the Society for Neuroscience *26*, 11474-11486.

Haacke, A., Broadley, S.A., Boteva, R., Tzvetkov, N., Hartl, F.U., and Breuer, P. (2006). Proteolytic cleavage of polyglutamine-expanded ataxin-3 is critical for aggregation and sequestration of non-expanded ataxin-3. Human molecular genetics *15*, 555-568.

Haacke, A., Hartl, F.U., and Breuer, P. (2007). Calpain inhibition is sufficient to suppress aggregation of polyglutamine-expanded ataxin-3. The Journal of biological chemistry *282*, 18851-18856.

Hirota, J., Ando, H., Hamada, K., and Mikoshiba, K. (2003). Carbonic

anhydrase-related protein is a novel binding protein for inositol 1,4,5-trisphosphate receptor type 1. The Biochemical journal *372*, 435-441.

Hsieh, M., Chang, W.H., Hsu, C.F., Nishimori, I., Kuo, C.L., and Minakuchi, T. (2013). Altered expression of carbonic anhydrase-related protein XI in neuronal cells expressing mutant ataxin-3. Cerebellum *12*, 338-349.

Huang, M.S., Wang, T.K., Liu, Y.W., Li, Y.T., Chi, T.H., Chou, C.W., and Hsieh, M. (2014). Roles of carbonic anhydrase 8 in neuronal cells and zebrafish. Biochimica et biophysica acta *1840*, 2829-2842.

Hubener, J., Weber, J.J., Richter, C., Honold, L., Weiss, A., Murad, F., Breuer, P., Wullner, U., Bellstedt, P., Paquet-Durand, F*., et al.* (2013). Calpain-mediated ataxin-3 cleavage in the molecular pathogenesis of spinocerebellar ataxia type 3 (SCA3). Human molecular genetics *22*, 508-518.

Jiao, Y., Yan, J., Zhao, Y., Donahue, L.R., Beamer, W.G., Li, X., Roe, B.A., Ledoux, M.S., and Gu, W. (2005). Carbonic anhydrase-related protein VIII deficiency is associated with a distinctive lifelong gait disorder in waddles mice. Genetics *171*, 1239-1246.

Kawaguchi, Y., Okamoto, T., Taniwaki, M., Aizawa, M., Inoue, M., Katayama, S., Kawakami, H., Nakamura, S., Nishimura, M., Akiguchi, I*., et al.* (1994). CAG expansions in a novel gene for Machado-Joseph disease at chromosome 14q32.1. Nature genetics *8*, 221-228.

Kaya, N., Aldhalaan, H., Al-Younes, B., Colak, D., Shuaib, T., Al-Mohaileb, F., Al-Sugair, A., Nester, M., Al-Yamani, S., Al-Bakheet, A*., et al.* (2011). Phenotypical spectrum of cerebellar ataxia associated with a novel mutation in the CA8 gene, encoding carbonic anhydrase (CA) VIII. American journal of medical genetics Part B, Neuropsychiatric genetics : the official publication of the International Society of Psychiatric Genetics *156B*, 826-834.

Kazachkova, N., Raposo, M., Montiel, R., Cymbron, T., Bettencourt, C., Silva-Fernandes, A., Silva, S., Maciel, P., and Lima, M. (2013). Patterns of mitochondrial DNA damage in blood and brain tissues of a transgenic mouse model of Machado-Joseph disease. Neuro-degenerative diseases *11*, 206-214.

Laco, M.N., Oliveira, C.R., Paulson, H.L., and Rego, A.C. (2012). Compromised mitochondrial complex II in models of Machado-Joseph disease. Biochimica et biophysica acta *1822*, 139-149.

Lee, G.S., Subramanian, N., Kim, A.I., Aksentijevich, I., Goldbach-Mansky, R., Sacks, D.B., Germain, R.N., Kastner, D.L., and Chae, J.J. (2012). The calcium-sensing receptor regulates the NLRP3 inflammasome through Ca^{2+} and cAMP. Nature 492, 123-127.

Macedo-Ribeiro, S., Cortes, L., Maciel, P., and Carvalho, A.L. (2009). Nucleocytoplasmic shuttling activity of ataxin-3. PloS one *4*, e5834.

Martina, M., Kilic, G., and Cherubini, E. (1994). The effect of intracellular Ca2+ on GABA-activated currents in cerebellar granule cells in culture. The Journal of membrane biology *142*, 209-216.

Matsumoto, M., Yada, M., Hatakeyama, S., Ishimoto, H., Tanimura, T., Tsuji, S., Kakizuka, A., Kitagawa, M., and Nakayama, K.I. (2004). Molecular clearance of ataxin-3 is regulated by a mammalian E4. The EMBO journal *23*, 659-669.

McCampbell, A., Taylor, J.P., Taye, A.A., Robitschek, J., Li, M., Walcott, J., Merry, D., Chai, Y., Paulson, H., Sobue, G.*, et al.* (2000). CREB-binding protein sequestration by expanded polyglutamine. Human molecular genetics *9*, 2197-2202.

Mueller, T., Breuer, P., Schmitt, I., Walter, J., Evert, B.O., and Wullner, U. (2009). CK2-dependent phosphorylation determines cellular localization and stability of ataxin-3. Human molecular genetics *18*, 3334-3343.

Picaud, S.S., Muniz, J.R., Kramm, A., Pilka, E.S., Kochan, G., Oppermann, U., and Yue, W.W. (2009). Crystal structure of human carbonic anhydrase-related protein VIII reveals the basis for catalytic silencing. Proteins *76*, 507-511.

Pressman, B.C. (1976). Biological applications of ionophores. Annual review of biochemistry *45*, 501-530.

Ravikumar, B., Vacher, C., Berger, Z., Davies, J.E., Luo, S., Oroz, L.G., Scaravilli, F., Easton, D.F., Duden, R., O'Kane, C.J.*, et al.* (2004). Inhibition of mTOR induces autophagy and reduces toxicity of polyglutamine expansions in fly and mouse models

of Huntington disease. Nature genetics *36*, 585-595.

Riess, O., Rub, U., Pastore, A., Bauer, P., and Schols, L. (2008). SCA3: neurological features, pathogenesis and animal models. Cerebellum *7*, 125-137.

Rosenberg, R.N. (1992). Machado-Joseph disease: an autosomal dominant motor system degeneration. Movement disorders : official journal of the Movement Disorder Society *7*, 193-203.

Saez, M.E., Ramirez-Lorca, R., Moron, F.J., and Ruiz, A. (2006). The therapeutic potential of the calpain family: new aspects. Drug discovery today *11*, 917-923.

Shimohata, T., Nakajima, T., Yamada, M., Uchida, C., Onodera, O., Naruse, S., Kimura, T., Koide, R., Nozaki, K., Sano, Y.*, et al.* (2000). Expanded polyglutamine stretches interact with TAFII130, interfering with CREB-dependent transcription. Nature genetics *26*, 29-36.

Simoes, A.T., Goncalves, N., Koeppen, A., Deglon, N., Kugler, S., Duarte, C.B., and Pereira de Almeida, L. (2012). Calpastatin-mediated inhibition of calpains in the mouse brain prevents mutant ataxin 3 proteolysis, nuclear localization and aggregation, relieving Machado-Joseph disease. Brain : a journal of neurology *135*, 2428-2439.

Sjoblom, B., Elleby, B., Wallgren, K., Jonsson, B.H., and Lindskog, S. (1996). Two point mutations convert a catalytically inactive carbonic anhydrase-related protein (CARP) to an active enzyme. FEBS letters *398*, 322-325.

Soong, B., Cheng, C., Liu, R., and Shan, D. (1997). Machado-Joseph disease: clinical, molecular, and metabolic characterization in Chinese kindreds. Annals of neurology *41*, 446-452.

Takahashi, T., Kikuchi, S., Katada, S., Nagai, Y., Nishizawa, M., and Onodera, O. (2008). Soluble polyglutamine oligomers formed prior to inclusion body formation are cytotoxic. Human molecular genetics *17*, 345-356.

Trottier, Y., Cancel, G., An-Gourfinkel, I., Lutz, Y., Weber, C., Brice, A., Hirsch, E., and Mandel, J.L. (1998). Heterogeneous intracellular localization and expression of ataxin-3. Neurobiology of disease *5*, 335-347.

Tsai, H.C., Su, H.L., Huang, C.Y., Fong, Y.C., Hsu, C.J., and Tang, C.H. (2014). CTGF increases matrix metalloproteinases expression and subsequently promotes tumor metastasis in human osteosarcoma through down-regulating miR-519d. Oncotarget *5*, 3800-3812.

Tsujinaka, T., Kajiwara, Y., Kambayashi, J., Sakon, M., Higuchi, N., Tanaka, T., and Mori, T. (1988). Synthesis of a new cell penetrating calpain inhibitor (calpeptin). Biochemical and biophysical research communications *153*, 1201-1208.

Turkmen, S., Guo, G., Garshasbi, M., Hoffmann, K., Alshalah, A.J., Mischung, C., Kuss, A., Humphrey, N., Mundlos, S., and Robinson, P.N. (2009). CA8 mutations cause a novel syndrome characterized by ataxia and mild mental retardation with predisposition to quadrupedal gait. PLoS genetics *5*, e1000487.

Wang, K.K. (1990). Developing selective inhibitors of calpain. Trends in pharmacological sciences *11*, 139-142.

Wang, T.K., Cheng, C.K., Chi, T.H., Ma, Y.S., Wu, S.B., Wei, Y.H., and Hsieh, M. (2014). Effects of carbonic anhydrase-related protein VIII on human cells harbouring an A8344G mitochondrial DNA mutation. The Biochemical journal *459*, 149-160.

Wen, F.C., Li, Y.H., Tsai, H.F., Lin, C.H., Li, C., Liu, C.S., Lii, C.K., Nukina, N., and Hsieh, M. (2003). Down-regulation of heat shock protein 27 in neuronal cells and non-neuronal cells expressing mutant ataxin-3. FEBS letters *546*, 307-314.

Winborn, B.J., Travis, S.M., Todi, S.V., Scaglione, K.M., Xu, P., Williams, A.J., Cohen, R.E., Peng, J., and Paulson, H.L. (2008). The deubiquitinating enzyme ataxin-3, a polyglutamine disease protein, edits Lys63 linkages in mixed linkage ubiquitin chains. The Journal of biological chemistry *283*, 26436-26443.

Yu, Y.C., Kuo, C.L., Cheng, W.L., Liu, C.S., and Hsieh, M. (2009). Decreased antioxidant enzyme activity and increased mitochondrial DNA damage in cellular models of Machado-Joseph disease. Journal of neuroscience research *87*, 1884-1891.

Zou, C., Wang, Y., and Shen, Z. (2005). 2-NBDG as a fluorescent indicator for direct glucose uptake measurement. Journal of biochemical and biophysical methods *64*, 207-215.
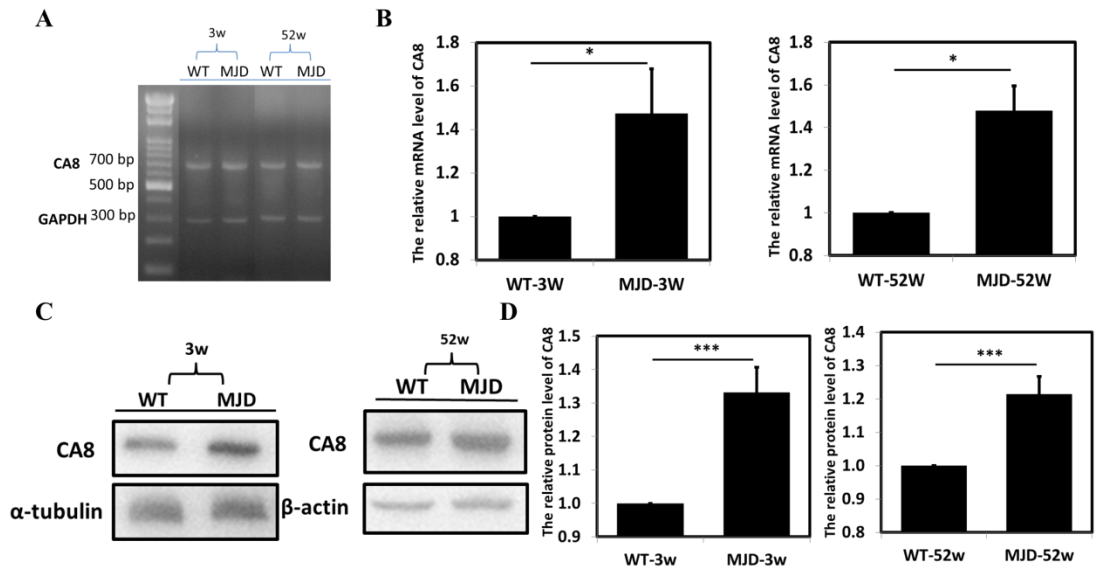
Figure 1.CA8 mRNA and protein analysis in wild type and SCA3/MJD transgenic mouse. (A) The mRNA levels were significantly higher in MJD Tg mice at 3weeks and 52weeks than those of WT. Total RNA from the different stages of mouse cerebellum was analyzed. The value of each experiment was from the average of triplicate PCR runs. (B) The quantified values were expressed as means ± SEM from four independent experiments. (*p<0.05) The value of each experiment was from the average of triplicate PCR runs. RT-PCR was performed using GAPDH primers as a control. (C) In Western blot analysis of CA8 expression in MJD Tg mice at 3weeks and 5weeks. CA8 protein level in MJD Tg mouse is higher than that of the wild type control. Expression of α-tubulin and β-actin was examined as a quantity control. (D) Data were expressed as means ± SEM from six separate experiments. * p<0.05. *** p< 0.001.
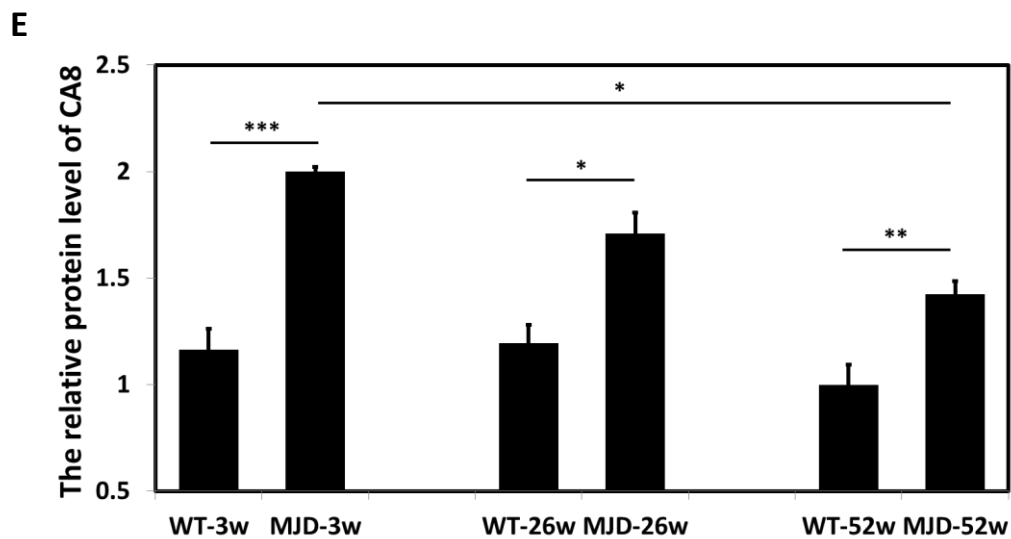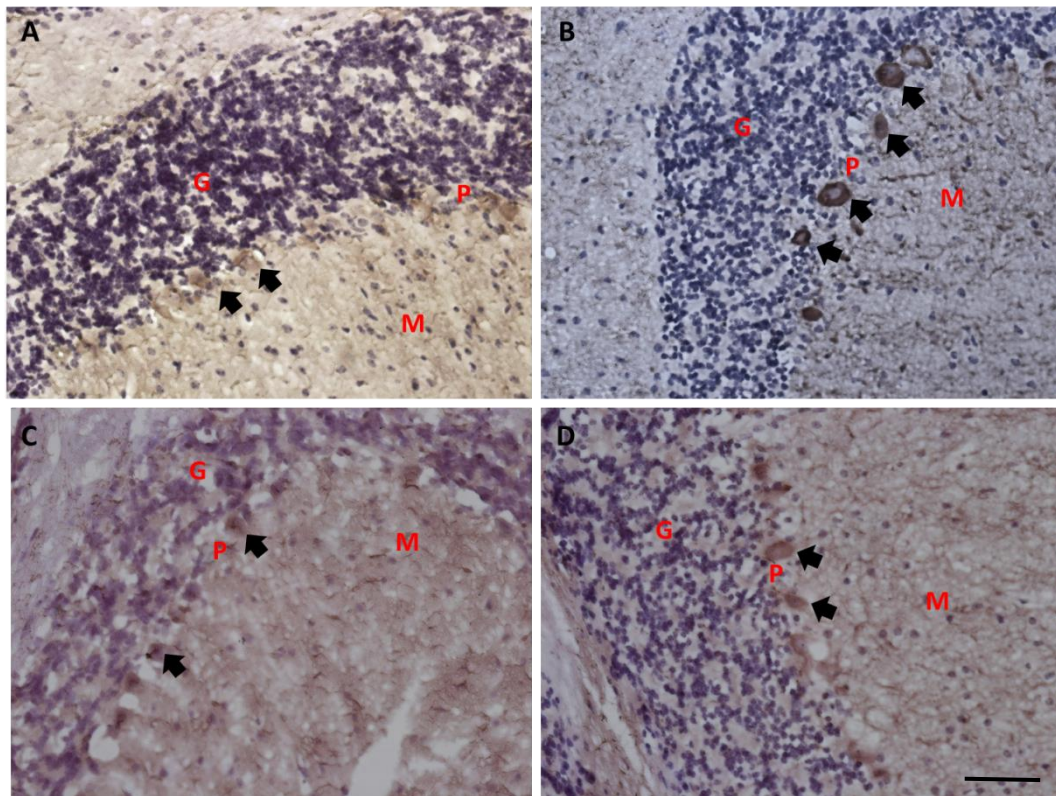
Figure 2.Immunohistochemistry of CA8 expression in the wild type and MJD Tg mice. CA8 was detected in Purkinje cells by immunohistochemistry (arrow sign) and the more intense staining was observed in MJD Tg mice of 3 weeks of age and 52 weeks (B and D), as compared with the control wild type (A and C). P:Purkinje cell layer, G:Granular cell layer, M:Molecular cell layer (E) The quantitative analysis indicated a significant increased CA8 expression in Purkinje cells of MJD mice at either 3 weeks (3w) or 52 weeks (52w), as compared with its wild type control. Data were expressed as Kruskal-Wallis test from six separate experiments. ** $p < 0.01$. *** $p < 0.001$.

A

B

C
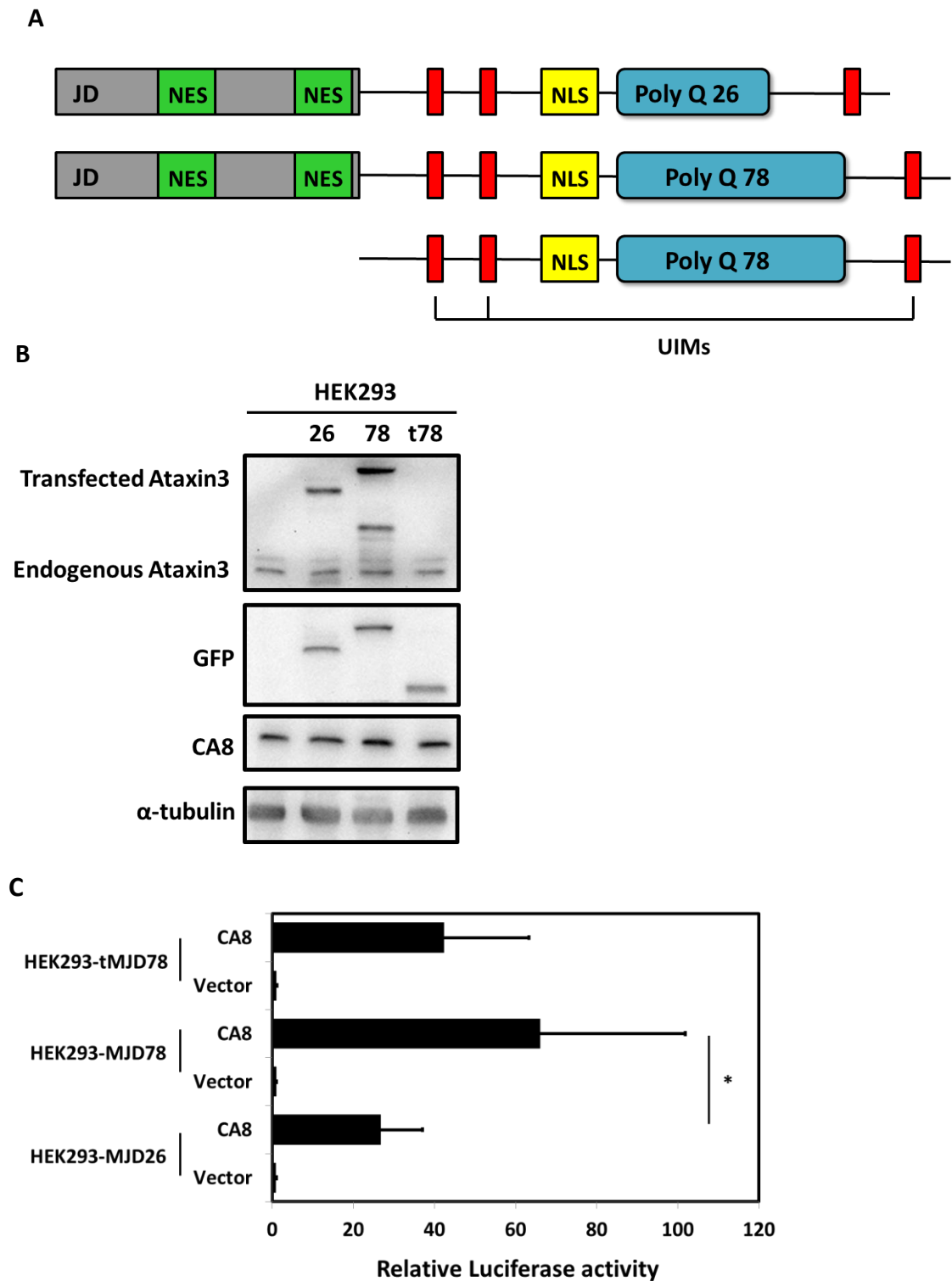
Figure 3.The ectopic expression of ataxin-3 and CA8 promoter activity in HEK293 cells. (A) A schematic diagram to illustrate three constructs containing ataxin-3 gene with 26 CAG repeats, 78 CAG repeats and N-terminal truncated 78 CAG repeats. NES and NLS are putative nuclear export and import signals, respectively. UIMs are ubiquitin-interacting motifs. (B) Western blot analysis of endogenous and exogenous ataxin-3 expression in HEK 293 cells. All the three plasmids are GFP-tagged. Western

blot analysis was performed by using antibodies against ataxin-3 or GFP. Expression of α-tubulin and β-actin was examined as a quantity control.

(C) Increased CA8 promoter activity in HEK293 cells harboring mutant ataxin 3. A construct containing the full-length of CA8 promoter region cloned into luciferase vector was co-transfected into HEK293 cell lines (HEK293-MJD26, HEK293-MJD78 and HEK293-tMJD78) along with a β-gal vector. The luciferase activity of HEK293-MJD78 was higher than HEK293-MJD26. Relative luciferase activity was calculated with respect to cells transfected with vector alone. Data were expressed as mean ± SEM of three independent experiments performed, each in duplicates. * $p < 0.05$.
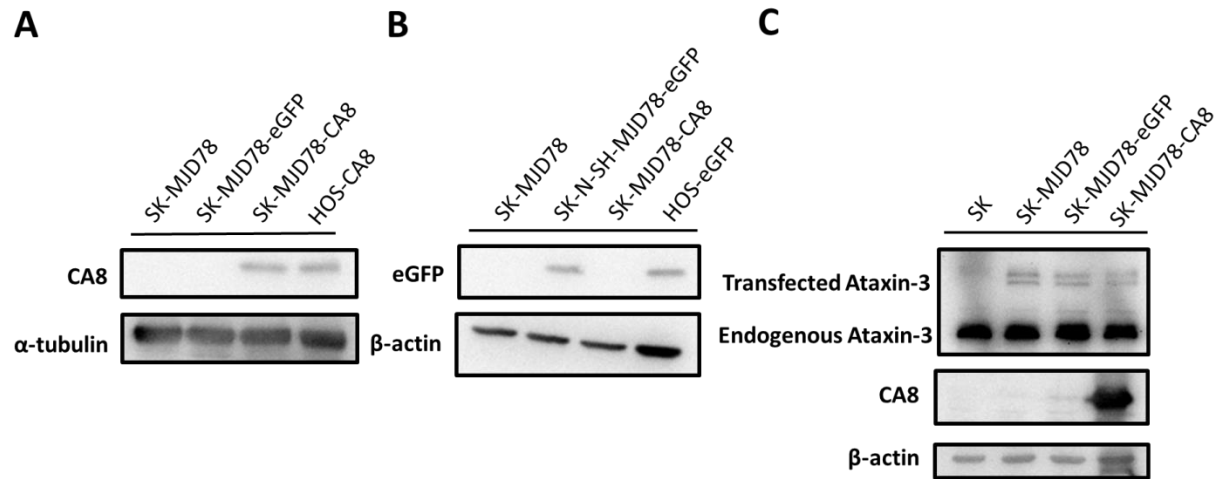
Figure 4.Protein expression of CA8 and ataxin-3 in SK-MJD78 cells with and without CA8 expression. (A) Western blot analysis of CA8 in SK-MJD78 cells with overexpression of CA8 and HOS-CA8 as a positive control.(B) Western blot analysis of CA8 in SK-MJD78 cells harboring overexpressing CA8 or eGFP. HOS- eGFP was used as a positive control for the signal of eGFP. (C) Western blot analysis of ataxin-3 in SK-N-SH, SK-MJD78, SK-MJD78-eGFP and SK-MJD78-CA8 cells. Endogenous ataxin-3(42k Da) and mutant ataxin-3(60k Da) were detected by antibodies against ataxin-3. Expression of α-tubulin and β-actin was examined for loading control.
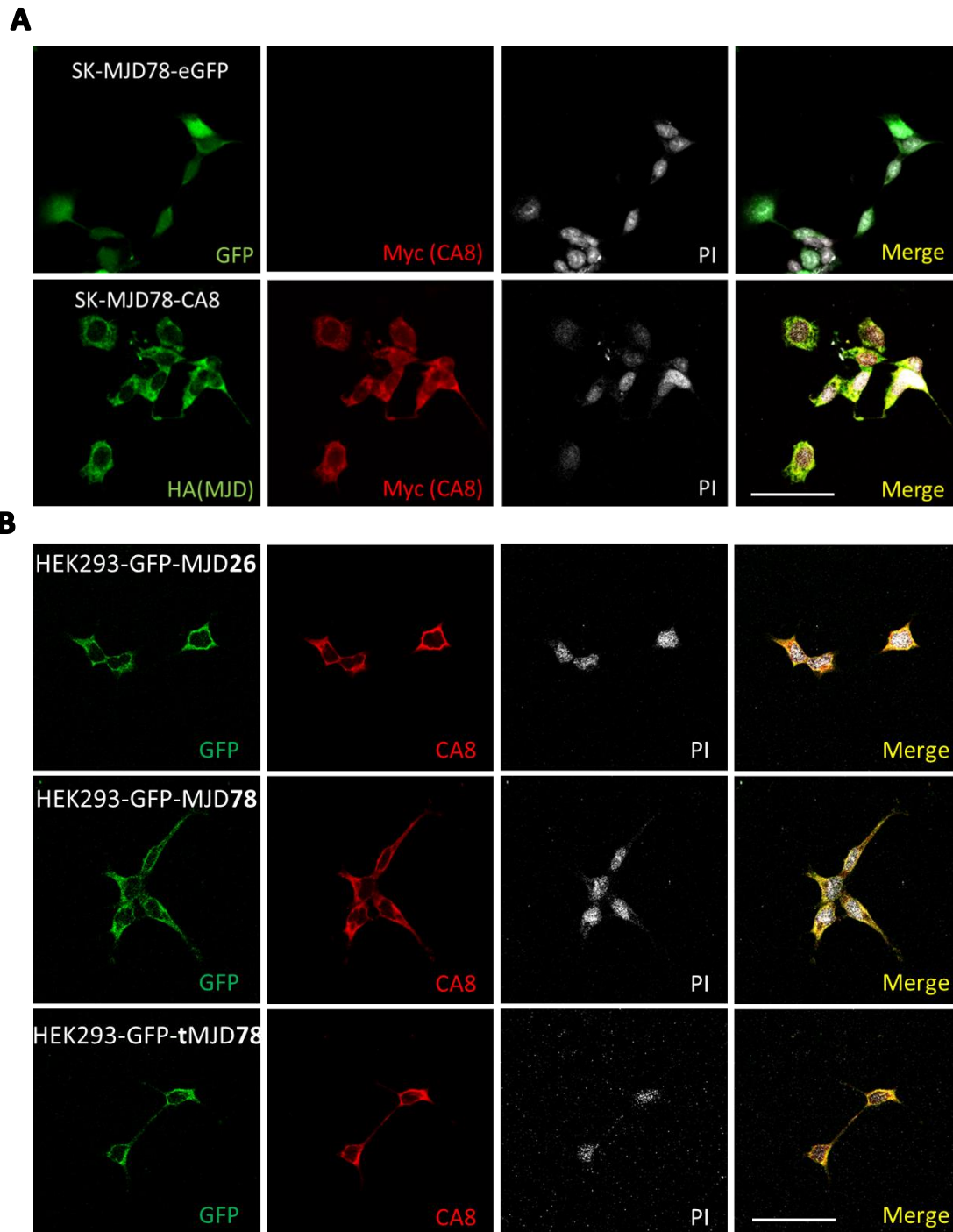
Figure 5. CA8 was co-localized with mutant ataxin-3 in SK-MJD78 cells with overexpressing CA8 (SK-MJD78-CA8) and HEK293 cell lines. (A) SK-MJD78-CA8 cells stably expressing HA-tagged mutant ataxin3 and together with myc-tagged CA8. SK-MJD78-eGFP cells stably expressing GFP. Double staining indicated colocalization (yellow) of Myc (green) and CA8 (red), scale bar, 50 μm. (B) HEK293 cells stably expressing GFP-tagged normal ataxin3 (HEK293-GFP-MJD26), mutant ataxin3 (HEK293-GFP-MJD78) and mutant ataxin3 lacking N-terminal (HEK293-GFP-tMJD78). Double staining indicated colocalization (yellow) of MJD (green) and CA8 (red), scale bar, 50 μm.
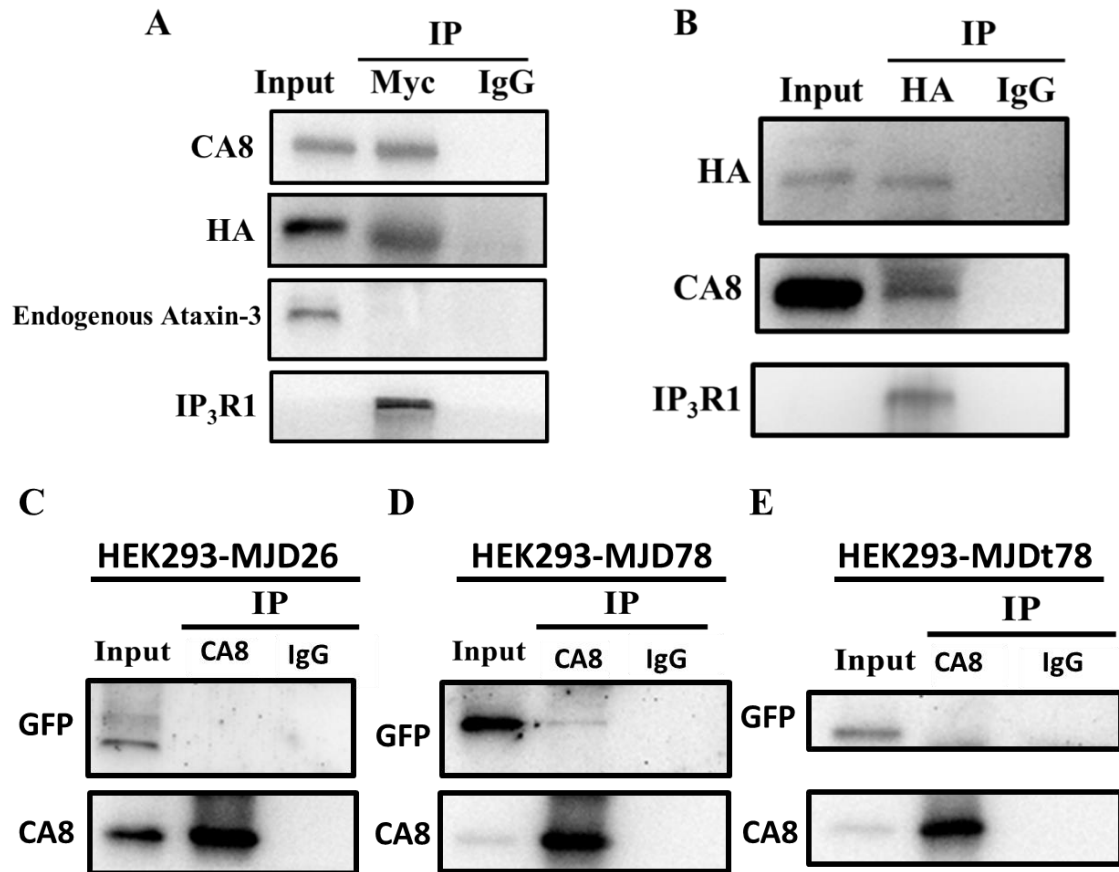
Figure 6.CA8 interacted with mutant ataxin-3 in SK-MJD78-CA8 and HEK293 cells stably expressing GFP-tagged mutant ataxin3 (HEK293-GFP-MJD78). (A) The cell lysates from SK-MJD78-CA8 were precipitated by anti-myc (CA8-tagged) and analyzed by Western blotting with anti-HA (MJD78-tagged). (B) The cell lysates from SK-MJD78-CA8 were precipitated by anti-HA and analyzed by Western blotting with anti-myc. The cell lysates from HEK293-MJD26 (C), HEK293-MJD78 (D) and HEK293-tMJD78 (E) were precipitated by anti-CA8 and analyzed by Western blotting with anti-GFP. The input lanes containing 1/50 of cell lysates was used for IP experiments. IgG was used as a negative control in the immunoprecipitation experiments.
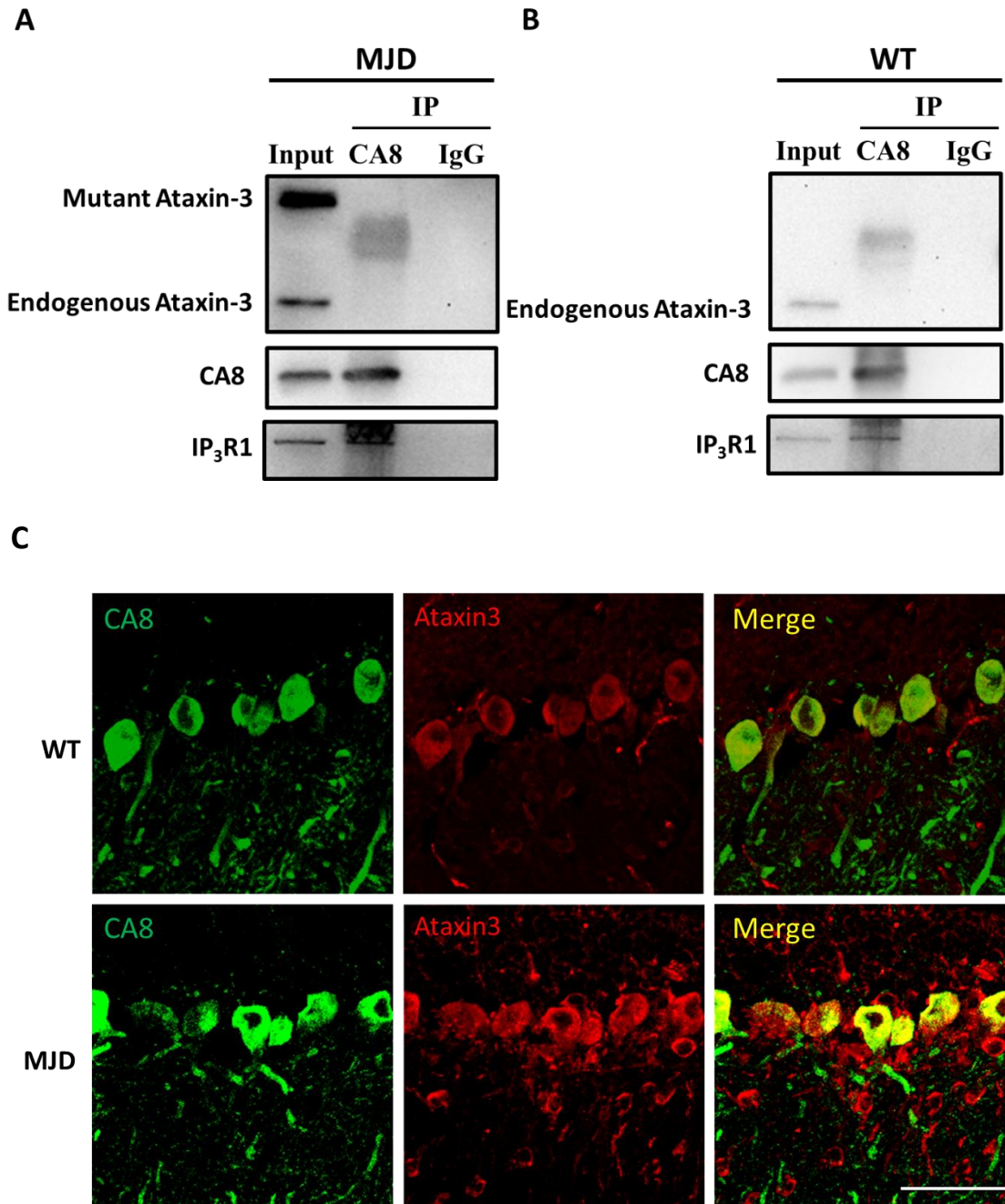
Figure 7.The interaction and localization between CA8 and mutant ataxin-3 in MJD Tg mouse model. (A) The cerebellum tissue lysates from MJD mouse were precipitated by anti-CA8 and analyzed by Western blotting with anti-Ataxin-3 and anti-IP$_3$R1. (B) The cerebellum tissue lysates from WT mouse were precipitated by anti-CA8 and analyzed by Western blotting with anti-Ataxin-3 and anti-IP$_3$R1. The input lanes contain 1/50 of cell lysates used for IP experiments. IgG was used as a negative control in the immunoprecipitation experiments. (C) CA8 was co-localized with mutant ataxin-3 in MJD Tg mouse model. Double staining indicated colocalization (yellow) of CA8 (green) and Ataxin-3 (red), scale bar, 50 μm.
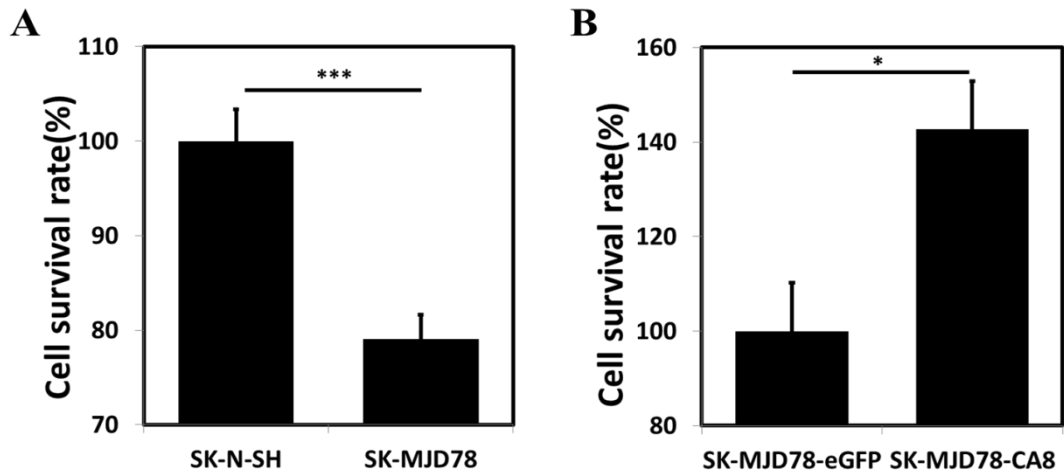
Figure 8. Overexpression of CA8 decreased cell death upon H_2O_2 treatment. (A) SK-N-SH cells showed increased cell survival than that in mutant SK-MJD78 cells. (B) SK-MJD78-CA8 cells were more resistant to oxidative stress as compared with that of SK-MJD78-eGFP cells. Data were expressed as means ± SEM from three separate experiments. * $p<0.05$. *** $p< 0.001$.
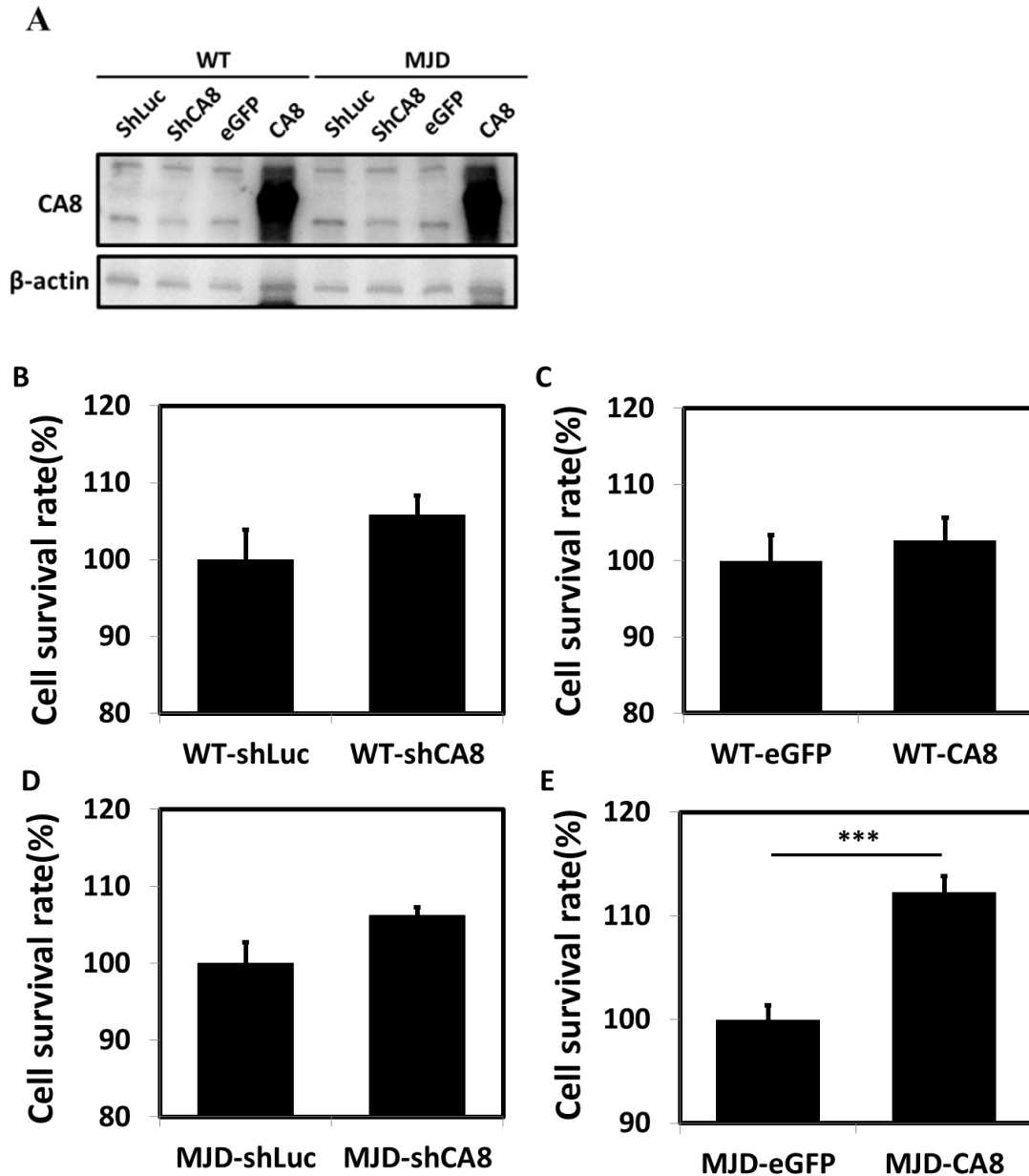
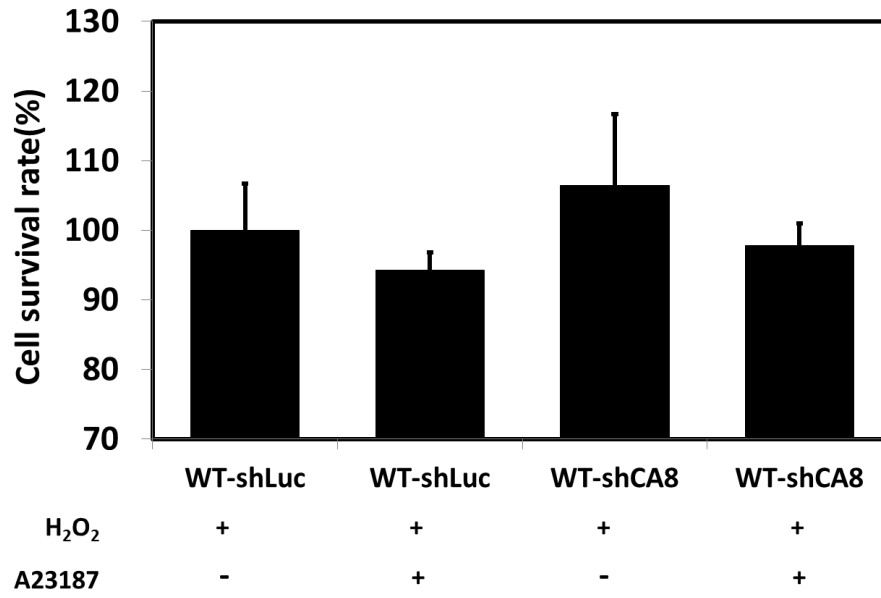Figure 9. Overexpression of CA8 in MJD CGNs increased cell survival upon H_2O_2 treatment. (A) Western blot analysis of CA8 in CGNs with down-regulated and overexpressing CA8. CGNs from wild type and MJD Tg mice were infected with CA8 shRNA lentivirus (shCA8), CA8 overexpression lentivirus (CA8), and control virus (eGFP and shLuc) according to the standard protocol. (B)(C) CGNs from wild type mouse with or without CA8 expression show no significant differences in cell survival. (D) CGNs from MJD Tg mouse with down-regulated CA8 showed no significant differences in cell survival. (E) MJD CGNs with overexpressing CA8 were more resistant to oxidative stress as compared with MJD CGNs with eGFP control. Data were expressed as means ± SEM from three separate experiments. *** p< 0.001.
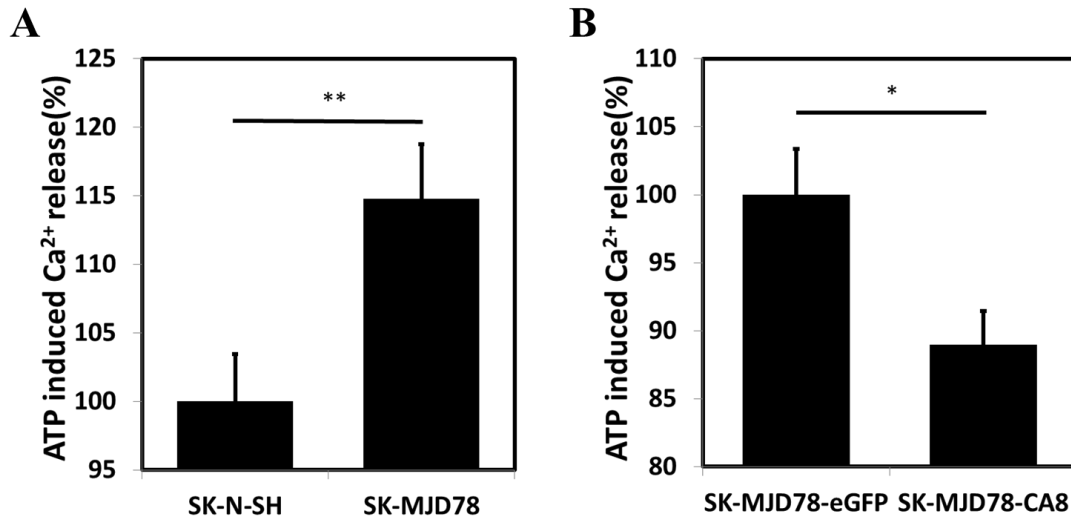
Figure 10.CA8 rescued abnormal Ca^{2+} release in SK-MJD78-CA8. Cytosolic calcium signals in response to 0.1 mM ATP. Fura-4M fluorescence was recorded continuously at 37℃ in a spectrofluorometer at excitation wavelength of 494 nm and an emission wavelength of 516 nm. (A) Increased Ca^{2+} release was observed in SK-MJD78 (mutant) cells as compared with that in SK-N-SH cells. (B) Overexpressing CA8 in SK-MJD78-CA8 cells decreased the abnormal Ca^{2+} release in SK-MJD78-eGFP cells. Data were expressed as means ± SEM from three separate experiments. * $p<0.05$. ** $p< 0.01$.
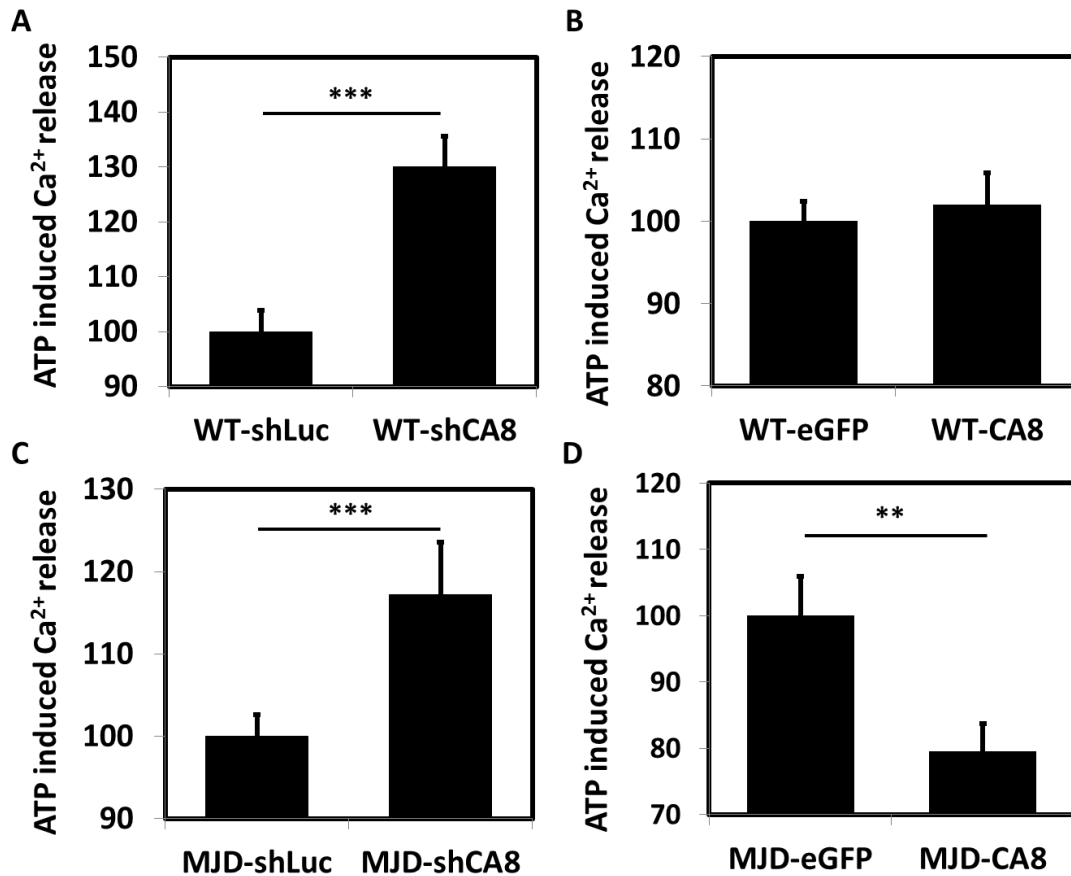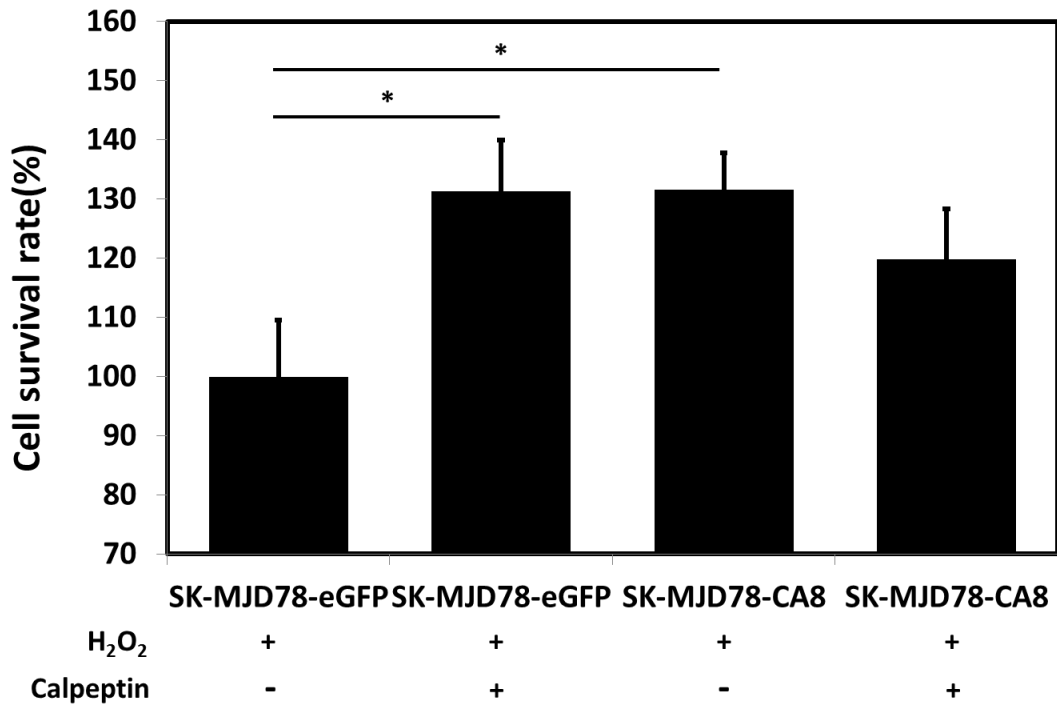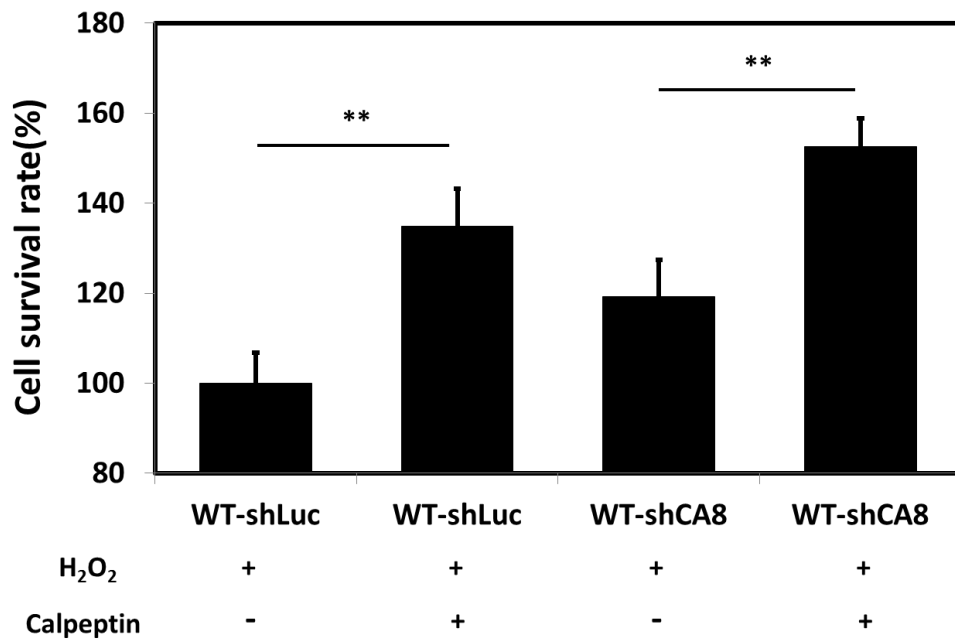
Figure 11. Decreased ER-dependent Ca^{2+} release in MJD CGNs with CA8 overexpression. CGNs from wild type and MJD mice were infected with CA8 shRNA lentivirus (shCA8), CA8 overexpression lentivirus (CA8), and control virus (eGFP and shLuc). Increased Ca^{2+} release was observed in both WT-shCA8 (A) and MJD-shCA8 (C) as compared with that of the control (shLUC). Overexpressing CA8 in WT cells showed no difference in calcium release as compared with that in WT-eGFP cells. (B). Overexpressing CA8 in MJD cells rescued the abnormal Ca^{2+} release in MJD-eGFP cells (D). Data were expressed as means ± SEM from three separate experiments. ** p<0.01. *** p< 0.001.

A

Cell survival rate(%)

	SK	SK	SK-MJD78	SK-MJD78
H$_2$O$_2$	+	+	+	+
A23187	-	+	-	+

B

Cell survival rate(%)

	SK-MJD78-eGFP	SK-MJD78-eGFP	SK-MJD78-CA8	SK-MJD78-CA8
H$_2$O$_2$	+	+	+	+
A23187	-	+	-	+

C

	WT-shLuc	WT-shLuc	WT-shCA8	WT-shCA8
H_2O_2	+	+	+	+
A23187	-	+	-	+

D

	WT-eGFP	WT-eGFP	WT-CA8	WT-CA8
H_2O_2	+	+	+	+
A23187	-	+	-	+
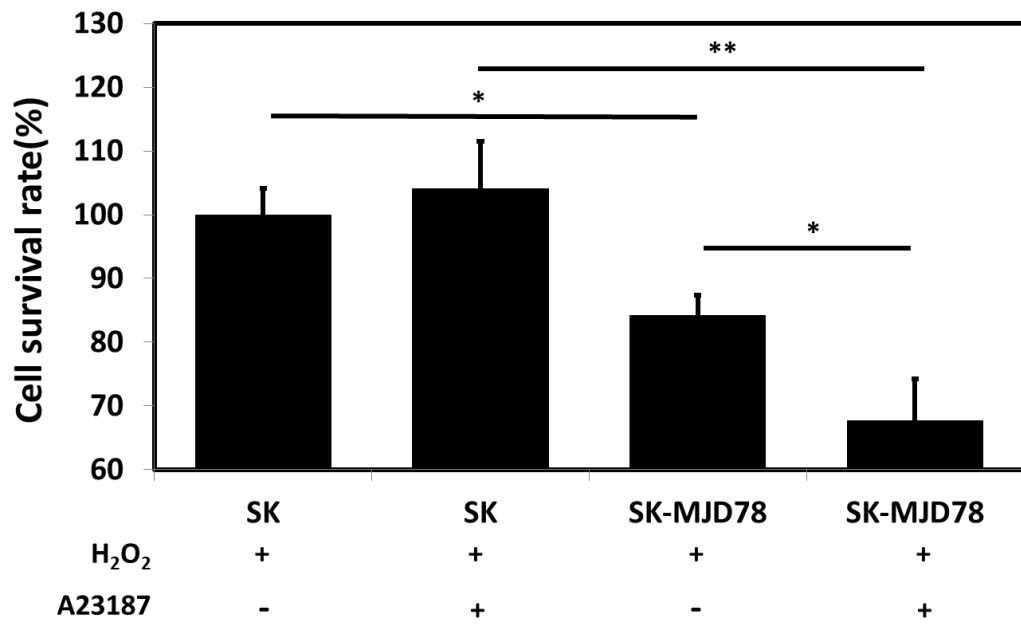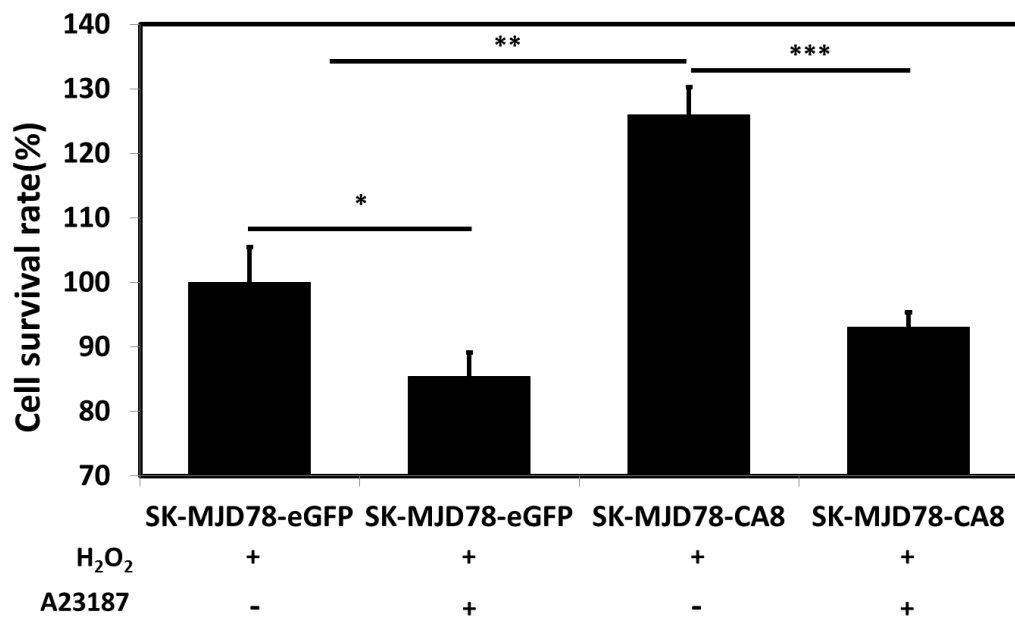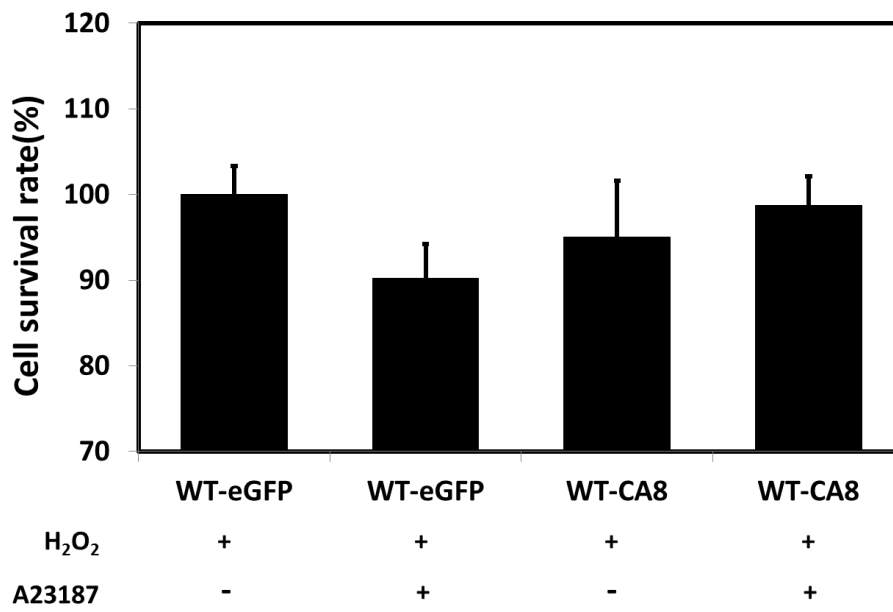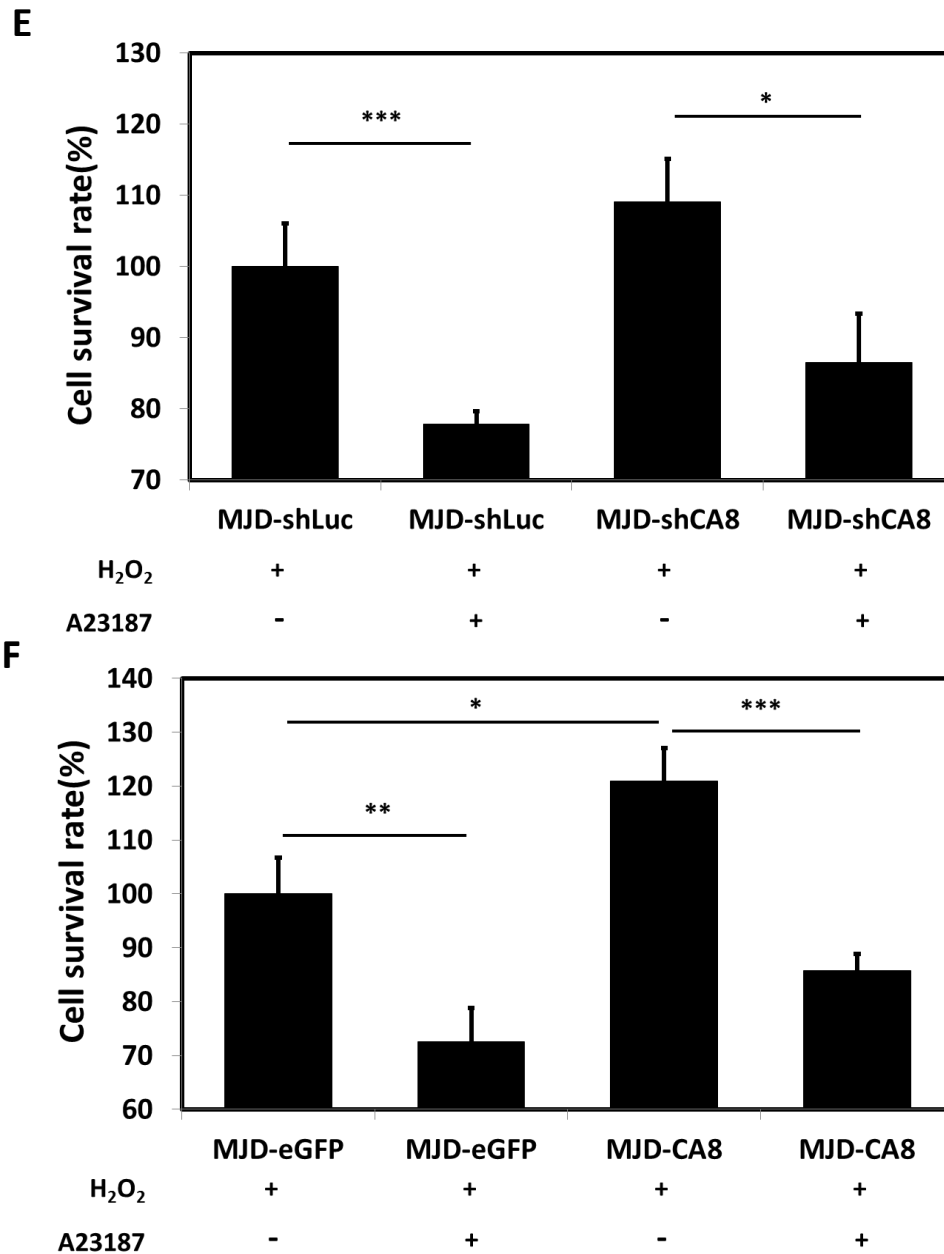
Figure 12. Ca^{2+} ionophore treatment (A23187) in SK-MJD78 cells and CGNs with or without CA8. (A) SK-MJD78 cells were more susceptible to oxidative stress and Ca^{2+} ionophore. (B) CA8 overexpression in SK-MJD78-CA8 induced more Ca^{2+} release and cell death as compared with that in SK-MJD78-eGFP (control) under Ca^{2+} ionophore (A23187) treatment. (C)(D) WT CGNs showed no significant difference in cells with or without CA8 uder Ca^{2+} ionophore treatment. (E) MJD-shLUC and MJD-shCA8 cells were more sensitive to oxidative stress by Ca^{2+} ionophore treatment (F) MJD-CA8 induced cell death under the Ca^{2+} ionophore treatment. Data were expressed as means ± SEM from three separate experiments. * p<0.05. ** p<0.01. *** p< 0.001.

68

A

B

E

Cell survival rate(%)

	MJD-shLuc	MJD-shLuc	MJD-shCA8	MJD-shCA8
H_2O_2	+	+	+	+
Calpeptin	-	+	-	+

F

Cell survival rate(%)

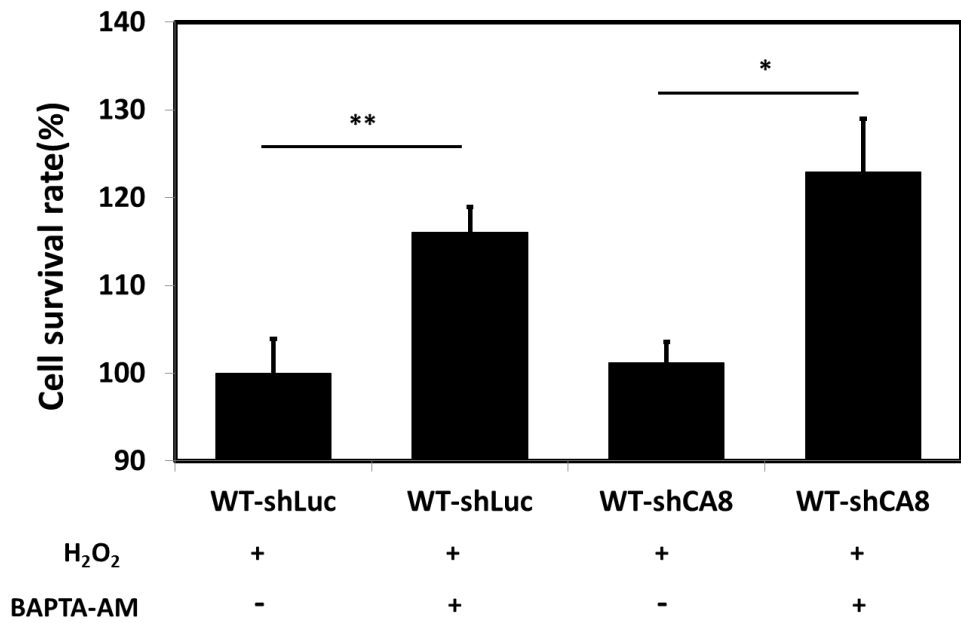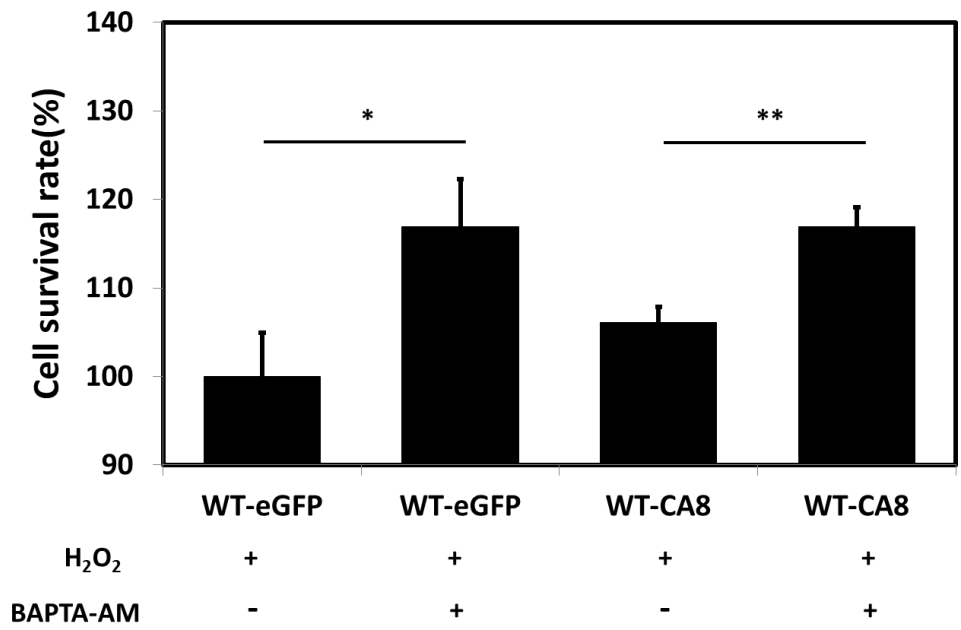|	MJD-eGFP	MJD-eGFP	MJD-CA8	MJD-CA8
H_2O_2	+	+	+	+
Calpeptin	-	+	-	+
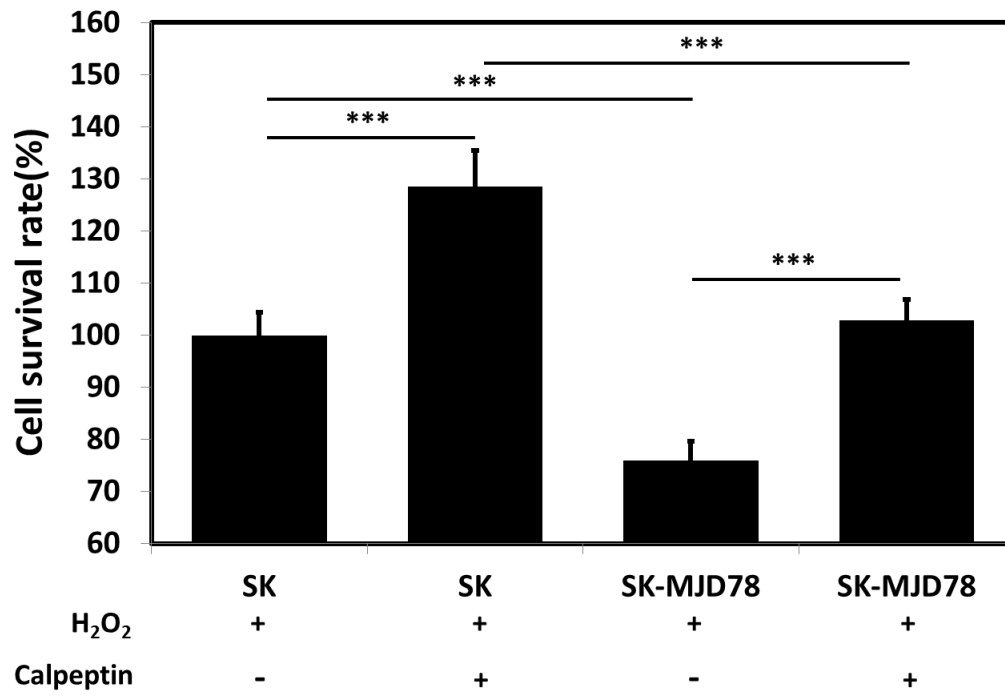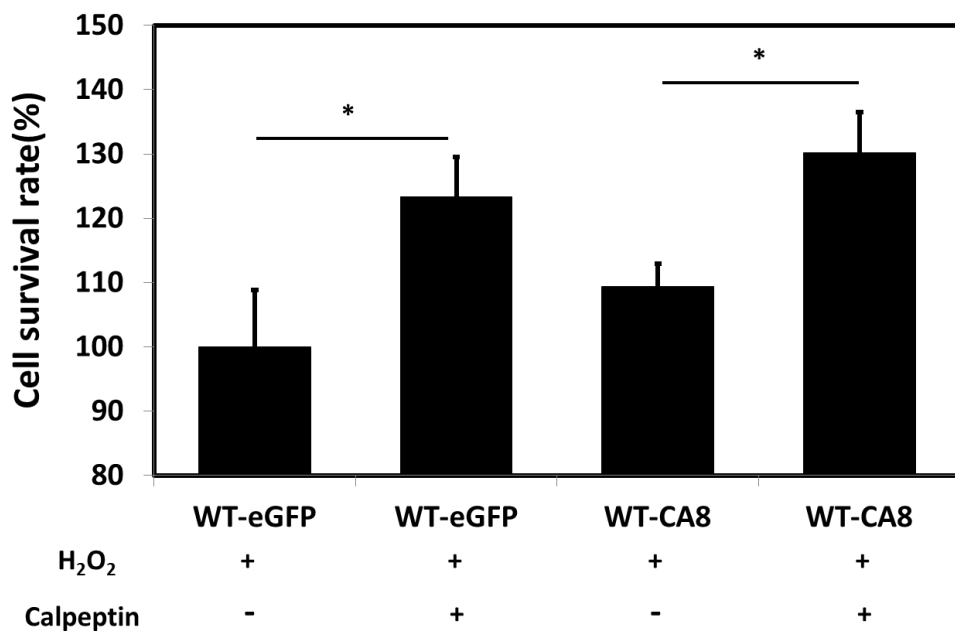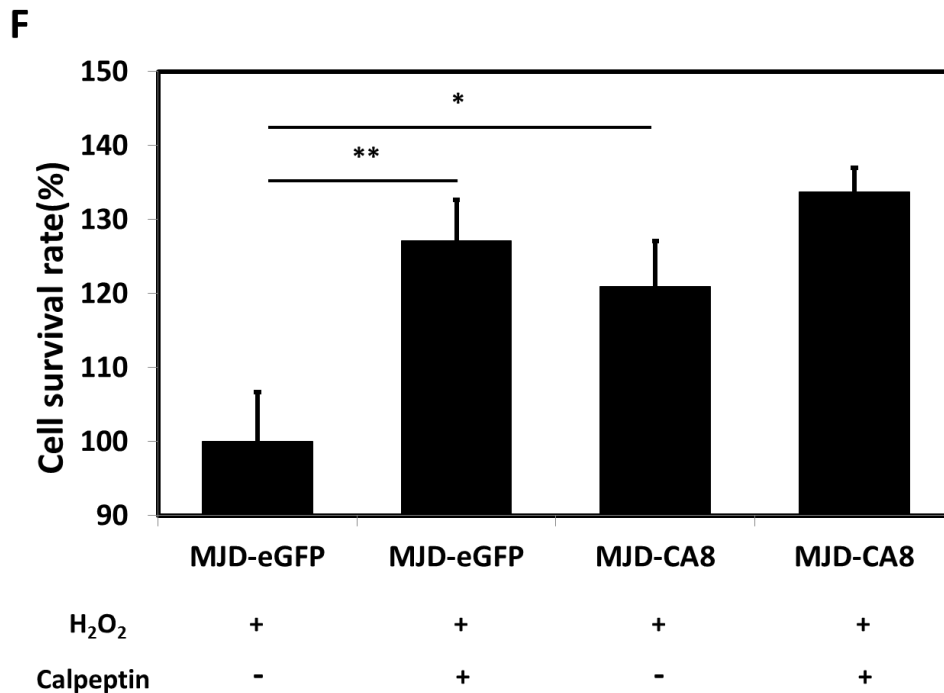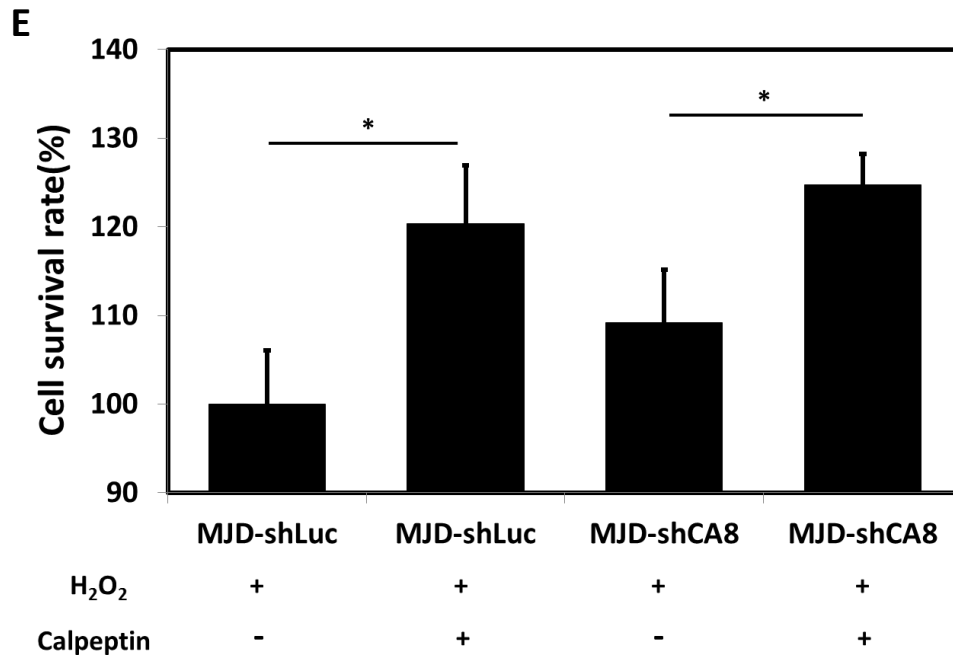
Figure 13. Calpeptin treatment in SK-N-SH cells, in CGNs with or without CA8. (A) Calpeptin reduced cell death in SK-MJD78 cells. (B) CA8 showed no effects on cell survival of SK-MJD78 cells with calpeptin treatment. (C)(D) Calpeptin increased cell survival under the calpeptin treatment in WT CGNs with or without overexpressing CA8. (E) Calpeptin increased cell survival under the treatment in MJD CGNs with knocked-down CA8. (F) Calpeptin increased cell survival under the treatment in MJD-eGFP and MJD-CA8 showed no effects on cell survival with calpeptin treatment. Data were expressed as means ± SEM from three separate experiments. * $p<0.05$. ** $p<0.01$. *** $p< 0.001$.
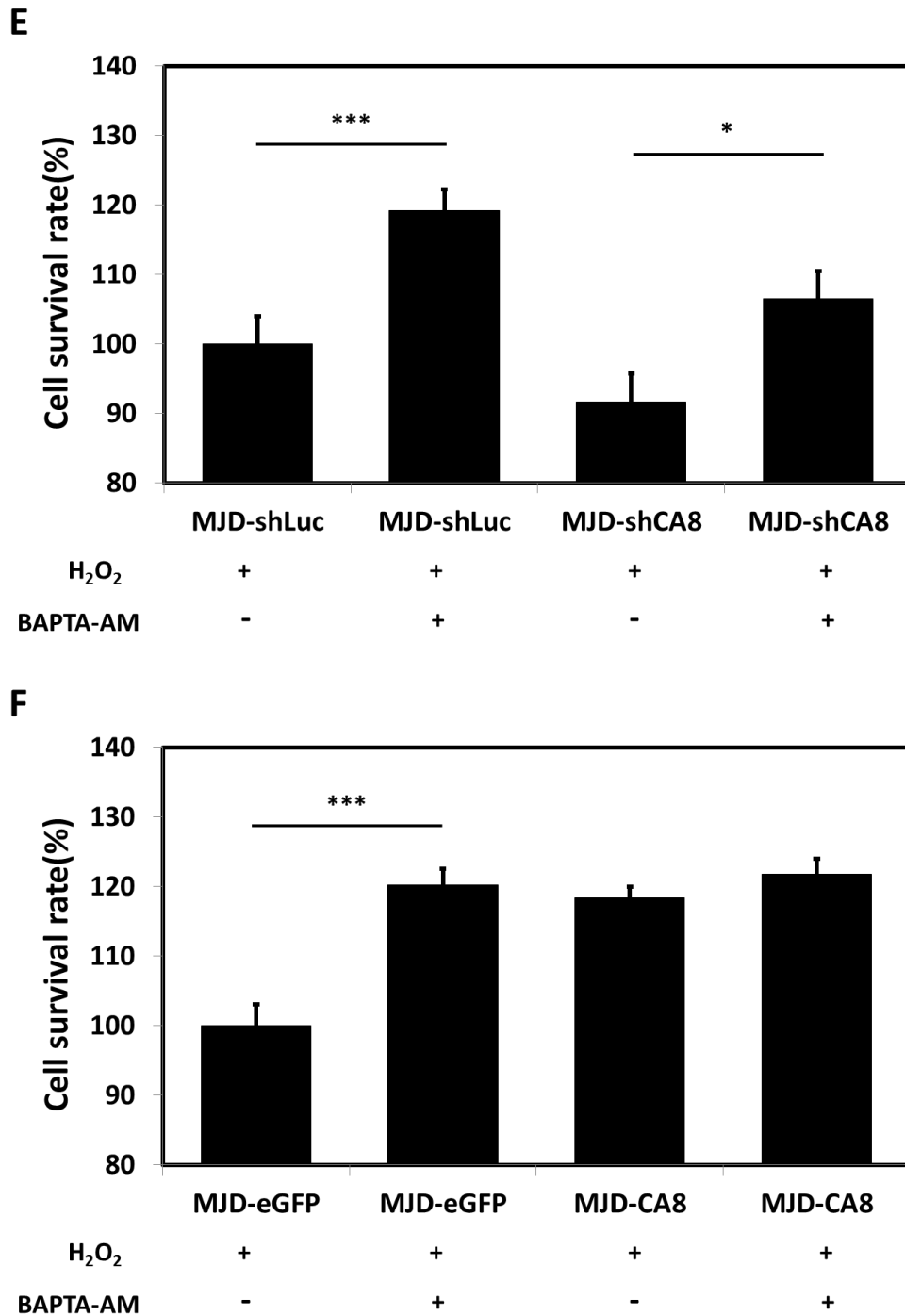
71

A

	SK	SK	SK-MJD78	SK-MJD78
H₂O₂	+	+	+	+
BAPTA-AM	-	+	-	+

B

	SK-MJD78-eGFP	SK-MJD78-eGFP	SK-MJD78-CA8	SK-MJD78-CA8
H₂O₂	+	+	+	+
BAPTA-AM	-	+	-	+

C

	WT-shLuc	WT-shLuc	WT-shCA8	WT-shCA8
H_2O_2	+	+	+	+
BAPTA-AM	-	+	-	+

D

	WT-eGFP	WT-eGFP	WT-CA8	WT-CA8
H_2O_2	+	+	+	+
BAPTA-AM	-	+	-	+
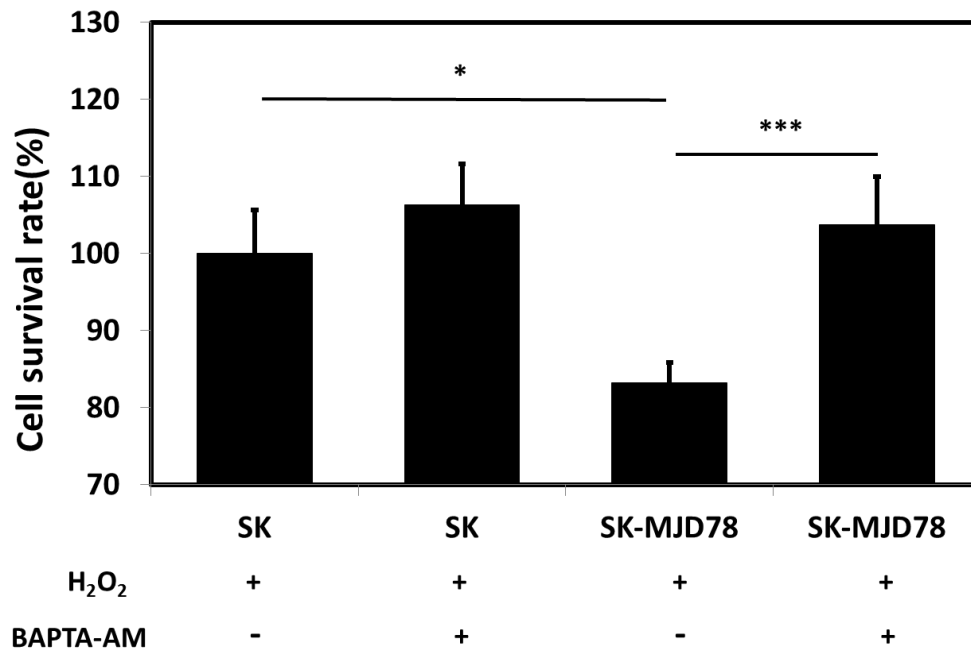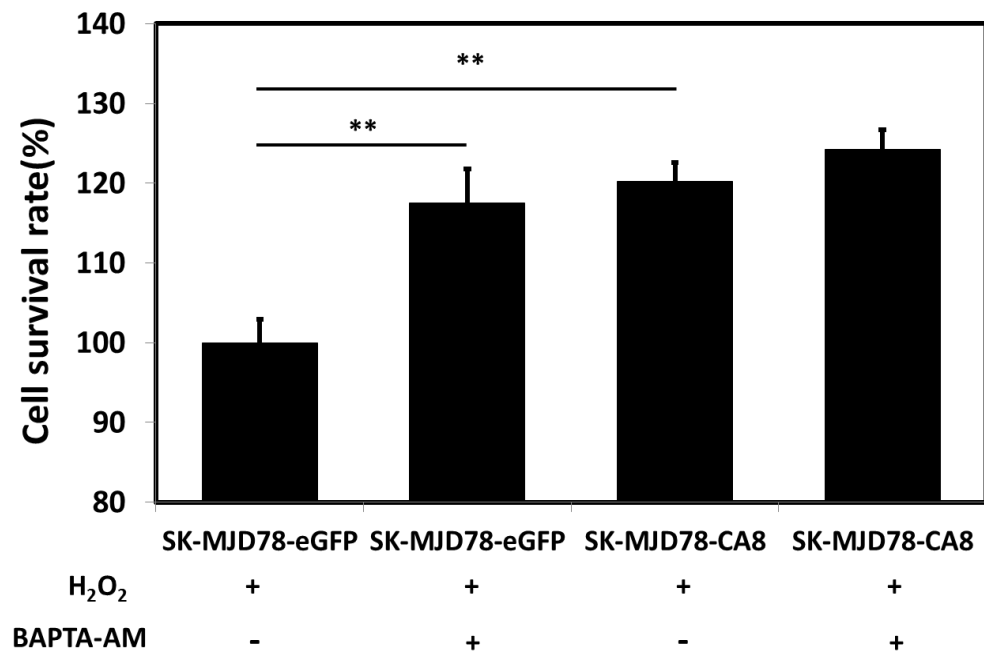
Figure 14. BAPTA-AM treatment in SK-N-SH cells and CGNs with different expression levels of CA8. (A) BAPTA-AM reduced cell death in SK-MJD78 cells. (B) CA8 shows no effects on cell survival in SK-MJD78 cells with BAPTA-AM treatment. (C)(D) BAPTA-AM increased cell survival in WT CGNs with or without CA8. (E) BAPTA-AM increased cell survival under H_2O_2 treatment in MJD CGNs with knocked-down CA8. (F) BAPTA-AM increased cell survival in MJD-eGFP but showed no effects on cell survival in MJD-CA8 cells. Data were expressed as means ± SEM from three separate experiments. * p<0.05. ** p<0.01. *** p< 0.001.
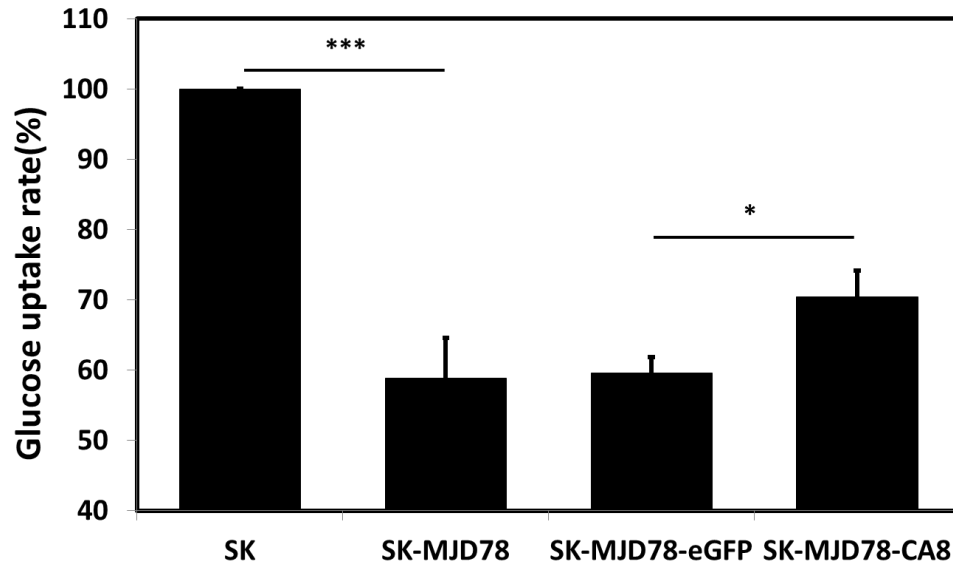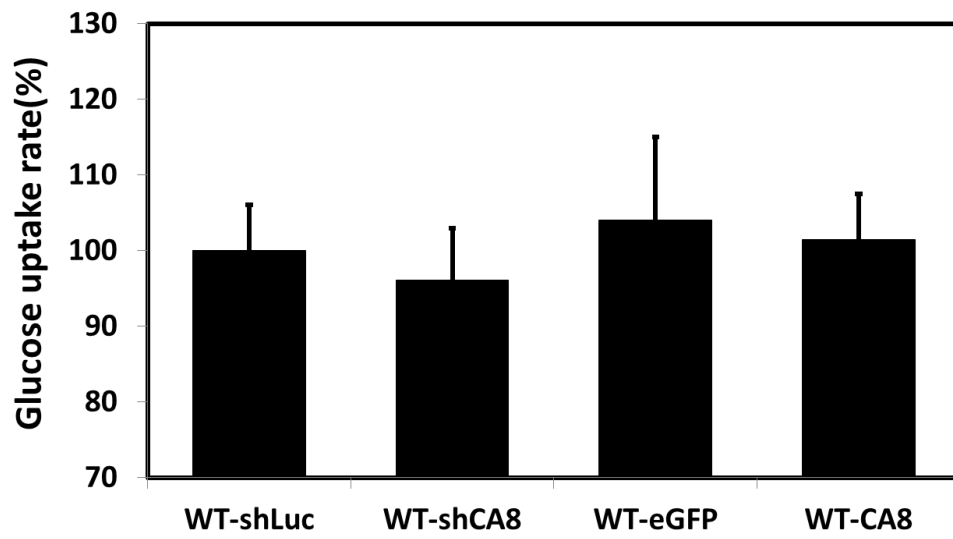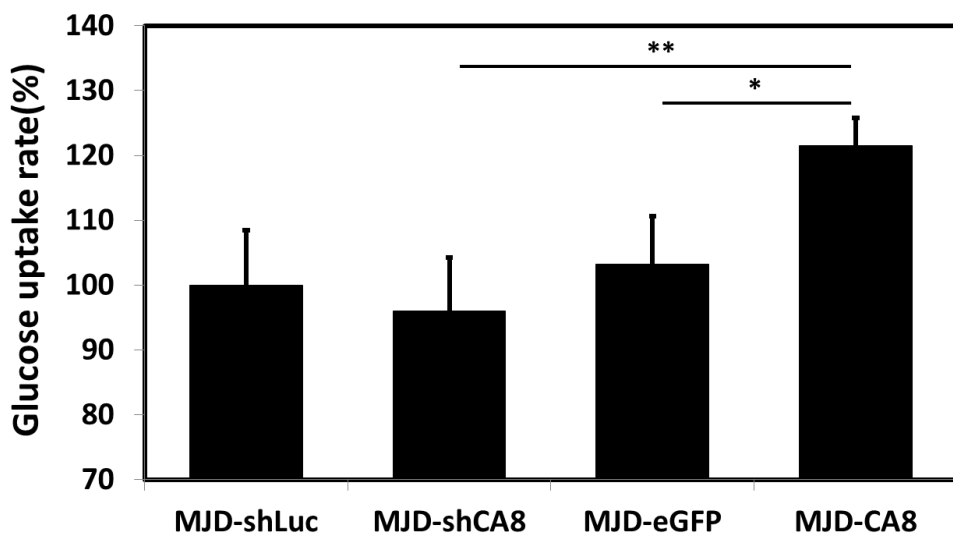
Figure 15. CA8 overexpression partially rescued glucose uptake in SK-MJD78-CA8 cells and in MJD CGNs with CA8 overexpression. (A) The glucose uptake rate of SK cells were significantly higher than SK-MJD78 cells. Overexpressing CA8 cells increased more glucose uptake than in SK-MJD78-eGFP cells. (B) In WT CGNs, there showed no significant different with or without CA8. (C) MJD-CA8 was partially increasing the glucose uptake compared to MJD-eGFP. Data were expressed as means ± SEM from three separate experiments. * $p<0.05$. ** $p<0.01$.
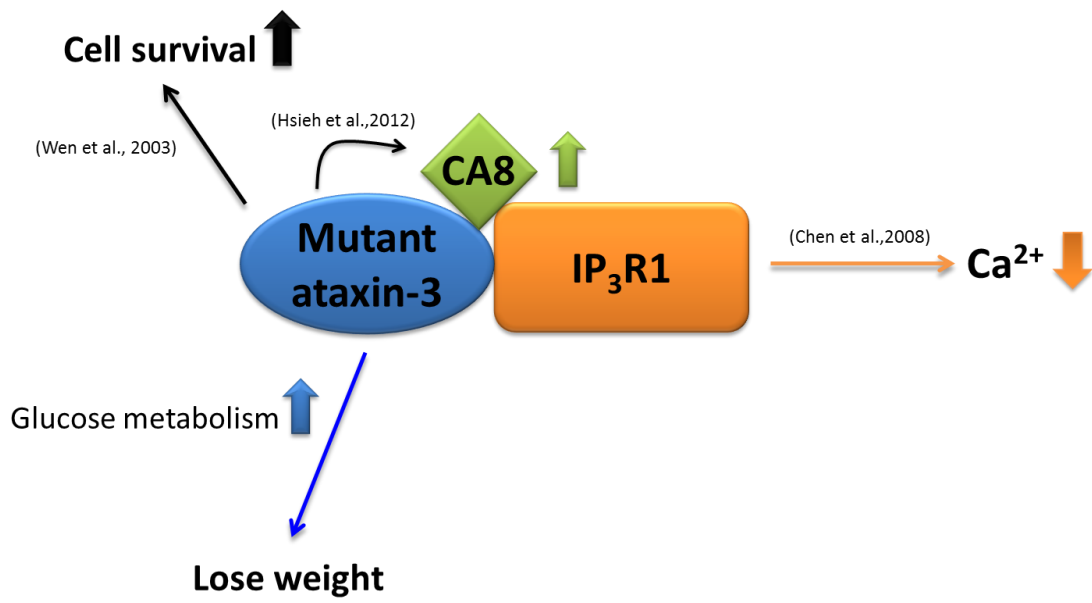
Figure 16. A model of the effects of CA8 in cells haboring mutant ataxin-3. In this model, CA8 interacts with mutant ataxin-3 and IP₃R1. In addition, overexpression of CA8 increases cell survival, decreases abnrmal ER-dependent Ca^{2+} release and partially rescues glucose uptake in MJD disease cells.
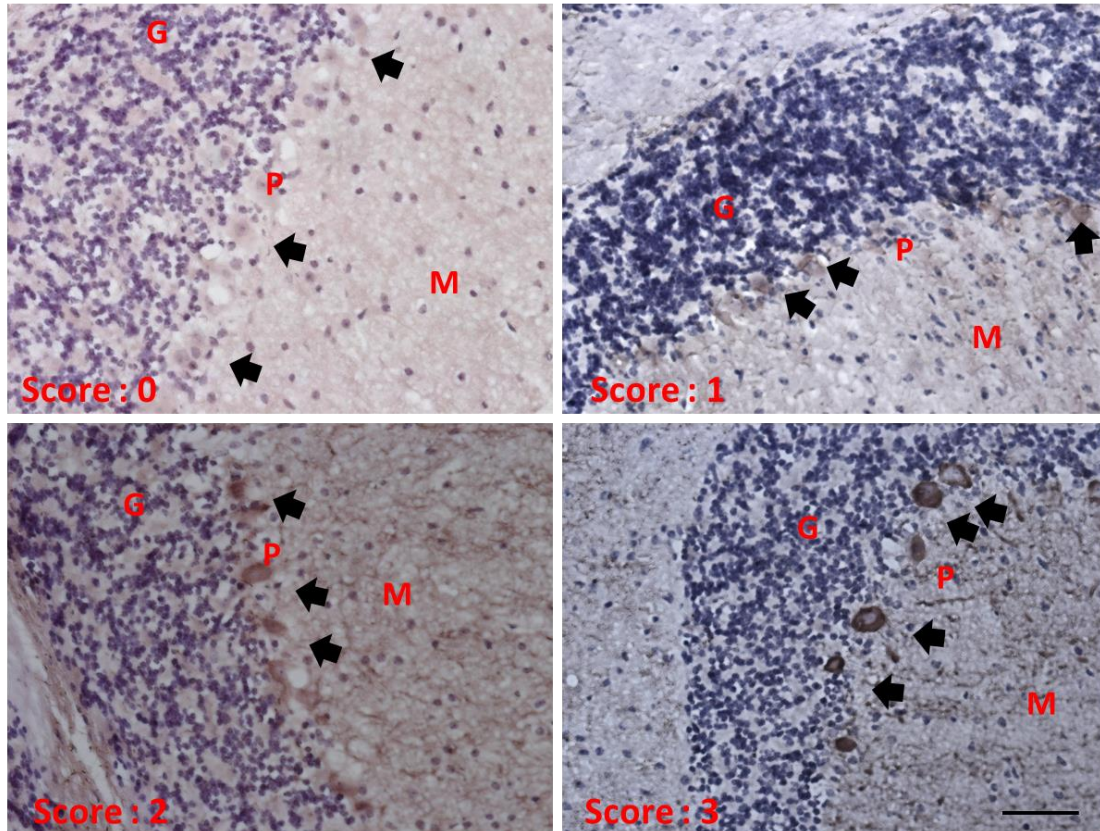
Figure S1. Representative figures to illustrate the definition of the IHC scoring to determine the CA8 expression. Each slide was assigned a score of 0 (no staining), 1 (slightly staining), 2 (moderately staining), or 3 (most intense staining) within Purkinje cells layers. P: Purkinje cell layer,   G: Granular cell layer, M: Molecular cell layer, scale bar, 50 μm.
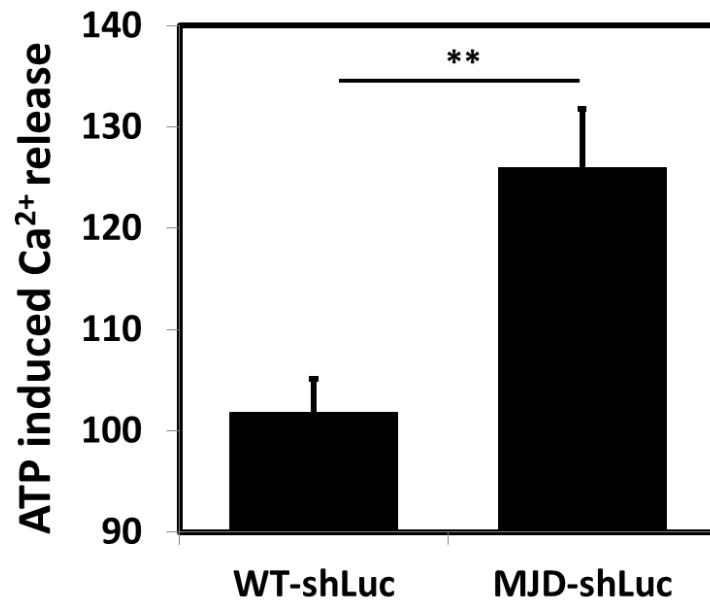
Figure S2. An increased Ca^{2+} release was observed in MJD CGNs infected with control virus (MJD-shLuc) as compared with that in WT CGNs infected with control virus (WT-shLuc).
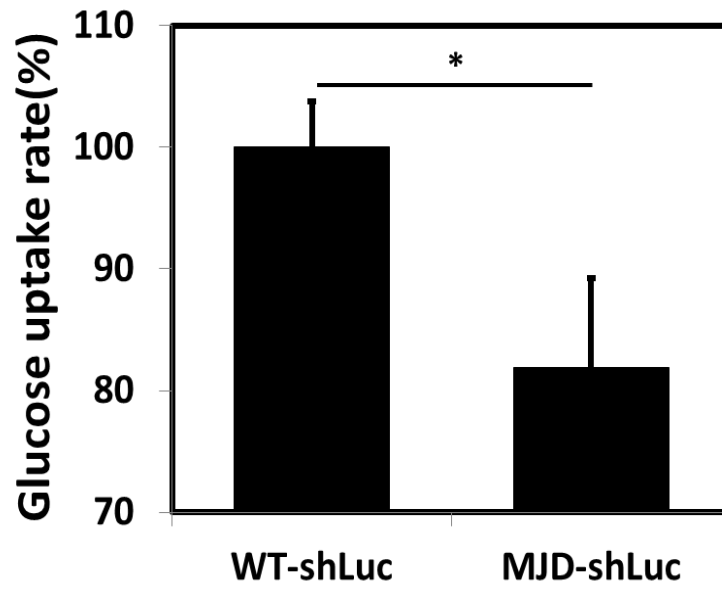
Figure S3. The glucose uptake of WT GCNs infected with control virus (WT-shLuc) was significantly higher than that of MJD GCNs infected with control virus (MJD-shLuc).

個人資料

中文姓名:李依庭

英文姓名:Yiting Li

戶籍地:台南市

出生日期:1990 年 12 月 15 日

電子郵件:r123734@gmail.com

學歷

2006-2009　私立聖功女子高級中學

2009-2013　私立東海大學生命科學系生物醫學組　學士

2013-2015　私立東海大學生命科學系生物醫學組　碩士

經歷

私立東海大學生命科學系分子生物學　助教